Western Graduate&PostdoctoralStudies

Western University
Scholarship@Western

Electronic Thesis and Dissertation Repository

7-18-2012 12:00 AM

Hypoxia-Induced Alterations in Skeletal Muscle Cell Respiration and Resveratrol as a Potential Pharmacological Intervention

Kathleen R. Belgrave
The University of Western Ontario

Supervisor
Dr. James F. Staples
The University of Western Ontario Joint Supervisor
Dr. Timothy R.H. Regnault
The University of Western Ontario

Follow this and additional works at: https://ir.lib.uwo.ca/etd

Part of the Physiology Commons

HYPOXIA-INDUCED ALTERATIONS IN SKELETAL MUSCLE CELL
RESPIRATION AND RESVERATROL AS A POTENTIAL PHARMACOLOGICAL
INTERVENTION

(Spine title: Hypoxic induced alterations in skeletal muscle respiration)

(Thesis format: Monograph)

by

Kathleen Rose <u>Belgrave</u>

Graduate Program in Biology

A thesis submitted in partial fulfillment
of the requirements for the degree of
Master of Science

The School of Graduate and Postdoctoral Studies
The University of Western Ontario
London, Ontario, Canada

THE UNIVERSITY OF WESTERN ONTARIO
School of Graduate and Postdoctoral Studies

CERTIFICATE OF EXAMINATION

Supervisor   Examiners

_____   _____
Dr. James Staples   Dr. Louise Milligan

_____
Dr. Timothy Regnault   _____
                                              Dr. Denis Maxwell

Supervisory Committee

                                              _____
                                              Dr. Greg Kelly
_____
Dr. Louise Milligan

_____
Dr. Jack Bend

The thesis by

Kathleen Rose <u>Belgrave</u>

entitled:

**Hypoxia-induced alterations in skeletal muscle cell respiration
and resveratrol as a pharmacological intervention**

is accepted in partial fulfillment of the
requirements for the degree of
Master of Science

_____   _____
            Date   Chair of the Thesis Examination Board

Abstract

Using the C_2C_{12} mouse muscle myoblast cell line, I sought to investigate the hypothesis that differentiation under hypoxia impairs muscle mitochondrial respiratory function irreversibly. Resveratrol (RSV) will increase expression of markers of mitochondrial biogenesis and reverse the hypoxia-induced depression of O_2 consumption rates. Hypoxia decreased oxygen consumption rates after five days of differentiation and after two days of normoxic recovery. This coincided with a hypoxia-induced decrease in protein levels of the NDUFB8 subunit of complex I of the electron transport chain and decreases in mRNA levels of mitochondrial biogenesis transcription factors, both of which could contribute to the alterations observed in oxygen consumption rates. Normoxic recovery supplemented with RSV did increase oxygen consumption rates, however this increase was not observed across all oxygen concentrations that were measured which may have be associated with the decreases in cell viability observed with RSV treatment. RSV also increased mitochondrial abundance which could account for the increases in oxygen consumption rate. RSV did increase some skeletal muscle markers of mitochondrial biogenesis, but did not increase protein levels of the subunit NDUFB8 of complex I. Hypoxia alters mitochondrial biogenesis and skeletal muscle respiratory function and may induce permanent changes in mitochondrial respiration of differentiating skeletal muscle cells. RSV treatment did not consistently reverse hypoxic alterations during normoxic recovery and negatively impacted cell viability indicating that RSV may not be a suitable pharmacological intervention for skeletal muscle cells which have differentiated under hypoxia.

Acknowledgements

I would first and foremost like to thank my supervisors, Dr. Tim Regnault and Dr. Jim Staples. Without your trust and support I would not have had this opportunity. I am not sure where I would have ended up without both of your leadership. I hope that I was able to set a stable groundwork for your future collaborations, it is the least I could do for everything that you have done for me. I could not be more grateful to have two supervisors who were consistently there for every question and problem I had. Beyond my research, you both made being a part of a lab an enjoyable experience and I have appreciated all of the laughs and, dare I say, friendship? Tim, make sure you tease all of your future students as much you have me, but remember, not everyone knows you are being sarcastic (I think it's the accent). Jim, be sure to hold more Grad Club meetings in the future, I know I always found them profoundly beneficial.

Next I would like to thank my committee. Your support through my graduate career was integral to my success. You were never afraid to push my boundaries of knowledge, and always made sure I was on top of my game. Thank you for guiding me through these past two years.

Lin Zhao, the master of the Physiology lab, almost everything I know I owe to you. I thank you for your never-ending patience and willingness to answer even the simplest of my questions. I am grateful for every tool and piece of knowledge you gave me to ensure I was a successful lab-worker. Walking into a new lab is intimidating, but you made it easy Lin. There are not enough words to thank you.

No graduate student is able to get through the day without a good support system. That support for me is my family. Mom, Dad, Kelly and Ryan, your encouragement and

support through my entire life has made me the person I am today. I owe all of my success to you. Thank you for teaching me how to stand on my own two feet and trusting me to follow my dreams and aspirations. I love you all so much.

I was lucky enough to work in two different labs during my graduate career. Let's start with the Staplers. How can I express how grateful I am that you always made sure I stayed humble with your sarcastic remarks? The laughs I shared with you guys were priceless and I thank you for always brightening my day. Jason Brown, I'll never forget that beard and your wit. Dillon Chung, we've been through this together from the beginning; from the disasters, to the failures, to the occasional good days. Thank you for always being a shoulder to whine on.

To the DDT lab, there are too many of you to thank individually, but I want you all to know that I don't think we should have as much fun in a lab as we do. From long days in the lab to nights out after conferences, you all always made sure that it was memorable. I don't think I would have made it through these past two years without such amazing people around to enjoy it with. I do have to single out Stephanie Hallows. Steph, I still don't remember when our friendship started, but I know our lab would have been much quieter if it never did. Thank you for the guidance you were always so willing to give me, and thank you for the screams, laughter and general silliness you brought into the lab each day.

Although this thesis is made up of plenty of my own blood sweat and tears, I owe my success to everyone who helped me or pushed me along these past two years. Without them, I would have never made it to where I am today. Thank you all so much.

Table of Contents

List of Figures

APPENDICES

List of Tables

List of Appendices

List of Abbreviations

AMPK	Adenosine monophosphate activated kinase
ATP	Adenosine triphosphate
CoA	Coenzyme A
CS	Citrate synthase
Cyt C	Cytochrome C
DCF	Dichlorofluorescein
DMEM	Dulbecco's modified Eagle's medium
D-PBS	Dulbecco's phosphate-buffered saline
ETC	Electron transport chain
FBS	Fetal bovine serum
HIF	Hypoxia-inducible factor
HS	Horse serum
IUGR	Intrauterine growth restriction
mtDNA	Mitochondrial DNA
NO	Nitric oxide
NRF	Nuclear respiratory factor
OXPHOS	Oxidative phosphorylation
PDH	Pyruvate dehydrogenase
PDHK	Pyruvate dehydrogenase kinase
PGC	Peroxisome proliferator-activated receptor gamma coactivator
PDE	Phosphodiesterase
Q	Coenzyme Q

qPCR	Quantitative polymerase chain reaction
RSV	Resveratrol
ROS	Reactive oxygen species
SIRT	Sirtuin
TCA	Tribcarboxylic acid cycle
Tfam	Mitochondrial transcription factor A
TFB1M	Mitochondrial transcription factor B1
TFB2M	Mitochondrial transcription factor B2
VDAC	Voltage-dependant channel

Chapter 1: Introduction

1.1 Developmental Origins of Health and Disease

Insulin resistance is a condition where peripheral tissues are unresponsive to the anti-lipolytic anabolic and glucose-lowering effects of insulin (Koves *et al*., 2008). It is associated with the development of the metabolic syndrome (Ford *et al*. 2002), a collection of diseases characterized by visceral obesity, dyslipidaemia, hyperglycaemia and hypertension (George *et al*., 2004), a major burden on our healthcare system today. Skeletal muscle, being a highly oxidative tissue, is a major site for carbohydrate and fatty acid metabolism (Schuler *et al*., 2006; Iossa *et al*., 2002), and the major peripheral tissue that is affected in insulin resistant individuals (Selak *et al*., 2003). Skeletal muscle of insulin resistant and Type II diabetic adults have lower levels of co-activators of mitochondrial biogenesis, smaller mitochondria and a decreased oxidative metabolic capacity when compared with healthy adults (Petersen *et al.* 2005; Patti *et al*., 2003; Kelley *et al*., 2002). Each of these studies indicate an association between decreased skeletal muscle bioenergetic capacity and the development of insulin resistance, and emerging evidence is showing that some insulin resistant adults may have been pre-programmed at birth.

A considerable body of evidence demonstrates that the *in utero* environment plays a major role in altering physiological and metabolic factors which pre-dispose individuals to the development of adult disease. Large population-based studies report that reduced prenatal growth leads to an increased risk for coronary heart disease, hypertension, higher cholesterol levels, insulin resistance and diabetes (De Boo and Harding, 2006; Barker *et al*., 1993; Barker *et al*., 1991). Maternal and fetal malnutrition was commonly found to be

the cause of abnormal fetal growth. From these studies, the term "thrifty phenotype" has frequently been used in reference to these smaller than average infants, referring to the idea that the fetus must make metabolic and physiological alterations due to an altered *in utero* environment (De Boo and Harding, 2006; Barker, 2004). These metabolic alterations may be irreversible, and prepare the fetus for an extrauterine life with the same poor environment (De Boo and Harding, 2006), such as low food availability. Currently, all perturbations to the fetus including maternal diet, utero-placental blood flow, placental function and fetal metabolism are considered to contribute to altering fetal development (Gillman, 2005).

Infants with a birthweight below the tenth percentile have an increased incidence of developing insulin resistance in adulthood compared to infants with an average birthweight (Jacquet *et al*., 2000). The World Health Organization estimates that in North America approximately 7% of births are low birthweight infants, while worldwide this figure increases to approximately 15% (World Health Organization, 2004). Animal models of restricted fetal growth display permanent changes in glucose homeostasis that ultimately leads to type 2 diabetes (Simmons *et al*., 2001), and these impairments are preceded by impaired mitochondrial oxidative metabolism in both liver and skeletal muscle (Peterside *et al*., 2003; Selak *et al.*, 2003). Increasing evidence links the development of insulin resistance in adulthood to these infants born underweight. Investigation into fetal programming of these dysfunctions may help elucidate the development of adult disease.

1.2 Hypoxia leading to altered skeletal muscle metabolism

1.2.1 Intrauterine growth restriction

The mammalian placenta maintains growth of the fetus by supplying nutrients and oxygen (O_2). Placental insufficiency, commonly caused by improper vascular development of the placenta, is characterized by low glucose and O_2 transfer and fatty acid and amino acid transport from maternal to fetal circulation (Baschat, 2004; Pardi *et al*., 2002). Decreases in placental transport result in fetal undernutrition and hypoxia (Cetin and Alvino, 2009; Pardi et al., 2002), thereby, impairing fetal growth. Fetuses with a birthweight which falls below the third percentile for gestational age and gender are deemed to be intrauterine growth restricted (IUGR; Baschat *et* al., 2006; Jaquet et al., 2000). The development of IUGR can be caused by a variety of maternal, placental and fetal factors including: fetal genetic diseases, toxic exposure such as smoking, and maternal malnutrition (Hendrix and Berghella, 2008). Placental insufficiency, however, is the most common cause of IUGR (Resnik, 2002).

The reduction in both nutrition and oxygenation can have profound effects on fetal development, but with increasing severity of hypoxia there is a proportional decrease in placental mass (Regnault *et al*., 2007), both of which are associated with an increased risk and severity of IUGR (Baschat, 2004; Strauss and Dietz, 1997). A decrease in O_2 supply has been shown to have detrimental effects on fetal growth distinct from insufficiencies in fetal nutrition (Giussani *et al*., 2007), highlighting hypoxia as a critical contributor to IUGR. Therefore, the focus of my thesis is on potential effects of hypoxia on muscle metabolism distinct from nutrition, furthering our understanding of hypoxia *in utero* and its effects on fetal growth.

1.2.2 Fetal developmental alterations under hypoxia

Under normal physiological conditions maternal capillary P_{O_2} can range from 80 - 100 mmHg (Ang *et al*., 1969), and fetal P_{O_2} in the umbilical vein can range from 20 - 30 mmHg (Lackman *et al.*, 2001). However, under IUGR conditions, the fetal P_{O_2} in the human umbilical vein blood may fall as low as 15 mmHg (Baschat *et al*., 2006; Lackman *et al*., 2001). Under both acute (Arbeille *et al*., 1995) and chronic (McLellan *et al*., 1992; Bristow *et al*., 1983) hypoxia, fetal blood flow is redistributed preferentially to vital organs such as the brain, heart and adrenals. Simultaneously, growth of peripheral tissues and organs, such as skeletal muscle is reduced (Sadiq, *et al*., 1999), to redistribute energy and O_2 to the growth of vital organs (McLellan *et al*., 1992). Finally under hypoxia there is also a reduction in O_2 consumption of skeletal muscle that is commonly associated with an increase in anaerobic metabolism (Bazaes *et al*., 2002; Bristow *et al.*, 1992). These alterations in metabolism in response to *in utero* hypoxia appear to persist following birth.

In a study that investigated glucose and lipid metabolism 48 hours after birth, IUGR infants had lower plasma glucose and insulin levels compared to average for gestational age infants (Bazaes *et al*., 2002). These infants had ample access to O_2 and nutrients during the 48 hour period, which suggested that the *in utero* alterations to glucose metabolism persisted after the insults of placental insufficiency were alleviated (Bazaes *et al*., 2002). The ability to alter development *in utero* to adjust to an insufficient environment can increase fetal survival, but can be accompanied by long-term complications postnatally (Joss-Moore *et al*., 2010). Tissues deprived of blood flow *in utero* by the redirection of blood and nutrients to spare vital organs at the expense of peripheral tissues, such as skeletal muscle, a major site for carbohydrate and fatty acid

metabolism (Schuler *et al*., 2006; Iossa *et al*., 2002), may be prone to these long term metabolic alterations.

1.2.3 Intrauterine growth restriction effects on skeletal muscle cell development

Various investigations have begun to highlight IUGR-associated alterations to skeletal muscle. Following an *in utero* hypoxic insult, rat IUGR offspring displayed a decrease in skeletal muscle cell respiration compared to controls, resulting in decreases in energy supply (Selak *et al*., 2003; Lane *et al.*, 1998). Furthermore, chronic hypoxic skeletal muscle studies reported decreased factors important for muscle mitochondrial biogenesis, such as Peroxisome proliferator-activated receptor gamma coactivator-1α (PGC-1α; Regnault *et al*., 2010). Decreases in mitochondrial biogenesis factors have also been observed *in vivo* in IUGR rats postnatally (Lane *et al*., 2003). These findings indicate that IUGR impacts skeletal muscle cell physiology prenatally resulting in altered skeletal muscle mitochondrial abundance and oxidative metabolism.

The fetal period is crucial for skeletal muscle development because no net increase in the number of muscle fibers occurs after birth (Zhu *et al.,* 2006); alterations which occur *in utero* could cause permanent changes to the IUGR infant. These IUGR animal models, however, display the compounding effects of both altered fetal nutrition and oxygenation by decreasing placental blood flow. A cultured system, C_2C_{12} cells derived from mice, closely parallel skeletal muscle differentiation from myoblasts to myotubes. Differentiated myotubes display decreases in O_2 consumption with decreasing O_2 tensions, suggesting that O_2 plays a role in regulating oxidative metabolism in developing skeletal muscle acutely (Arthur *et al*., 2000). However, the effect of chronic

hypoxia has not been extensively researched in this culture system. Therefore, examining the effects of chronic hypoxia on skeletal muscle mitochondria and oxidative metabolism can provide insight into fetal development under IUGR conditions, and may begin to elucidate how these individuals are pre-disposed to insulin resistance and, ultimately, the metabolic syndrome.

1.3 Mitochondrial function under normal physiological conditions

1.3.1 Mitochondrial oxidative phosphorylation

Oxidative phosphorylation (OXPHOS) is an important process which produces the majority of cellular energy in the form of adenosine triphosphate (ATP). Mitochondrial OXPHOS is dependent on the substrate upstream of the electron transport chain (ETC) and the ETC itself. Under normoxia, the products of glycolysis, fatty acid oxidation and amino acid oxidation are ultimately metabolized to acetyl-coenzyme A (CoA), which can be oxidized by the tricarboxylic acid (TCA) cycle within the mitochondrial matrix (Scarpulla, 2008; Kim *et al*., 2006). NADH and $FADH_2$ are produced during the TCA cycle and these molecules can then be oxidized by the ETC to initiate OXPHOS.

The ETC is embedded in the inner mitochondrial membrane and is composed of five complexes: NADH dehydrogenase (complex I), succinate dehydrogenase (complex II), cytochrome C reductase (Complex III), cytochrome C oxidase (Complex IV) and ATP synthase (complex V; Figure 1.1; Scarpulla, 2008). The ETC involves both the flow of electrons by a series of reduction and oxidation events and generation of a proton gradient. Electrons can be introduced to the ETC at complex I and complex II. Complex I

is reduced by the oxidation of NADH and complex II is reduced by oxidizing succinate (formed by the TCA cycle) or $FADH_2$. These electrons are passed along the complexes of the ETC by a series of oxidizing and reducing events, causing the release of free energy, which ends at complex IV, where the electrons reduce ½ O_2 molecule to produce H_2O (Figure 1.1). This release of free energy with the flow of electrons is used to pump H+ protons across the inner mitochondrial membrane to the intermembrane space, producing an electrochemical gradient across the inner membrane. Dissipation of this proton gradient through complex V drives the production of the high energy phosphate bonds of ATP when free ADP is present (Scarpulla, 2008).

1.3.2 Mitochondrial biogenesis

The biogenesis of functional mitochondria is dependent on both nuclear and mitochondrial DNA (mtDNA). A total of thirteen proteins are encoded by mtDNA, each essential subunits for the inner mitochondrial membrane complexes of the ETC (Scarpulla, 2008). The rest of the ETC subunits and other mitochondrial functional components are transcribed by nuclear genes. A network of nuclear-encoded transcription factors regulates the coordinated expression of nuclear and mtDNA encoded genes necessary for proper transcription and replication of mitochondria (Scarpulla, 2008).

The PGC-1 family of co-activators, including PGC-1α and PGC-1β, are major transcriptional co-regulators that can initiate the mitochondrial biogenesis program in cells in response to environmental stimuli (Handschin and Spiegelman, 2006; Finck and Kelly, 2006). Over-expression of PGC-1α/β has been associated with increases in mitochondrial number and increased expression of the mitochondrial regulatory

transcription factors NRF-1 and NRF-2α (nuclear respiratory factors 1 and 2; Figure 1.2; Scarpulla, 2006; Gleyzer *et al*., 2005). In addition to increasing the expression of these transcription factors, PGC-1α can also dock with them to activate promoters of mitochondrial genes (Scarpulla, 2006; Gleyzer *et al*., 2005). Specifically, NRF-1 and NRF-2α enhance the expression of nuclear-encoded subunits of the ETC (Figure 1.2 Scarpulla, 2006). Furthermore, they also act on the promoters of genes encoding transcription factors for mtDNA (Kelly and Scarpulla, 2004) such as mitochondrial transcription factor A (Tfam), mitochondrial transcription factor B1 (TFB1M) and mitochondrial transcription factor B2 (TFB2M; Scarpulla, 2008). Tfam is a high mobility group box protein that is an enhancer of mtDNA transcription and essential for mitochondrial replication because it contributes to the stabilization of mtDNA and increasing mtDNA copy number (Scarpulla 2006; Gleyzer *et al*., 2005). TFB2M contributes to mtDNA transcription by promoter recognition and increases mtDNA copy number for mitochondrial replication (Cotney *et al*., 2007; Scarpulla, 2006). TFB1M, in contrast to Tfam and TFB2M, only contributes to transcription of mtDNA by promoter recognition, and is markedly less active than TFB2M in this transcriptional stimulation (Cotney *et al*., 2007; Gleyzer *et al*., 2005). Each of these co-activators and transcription factors are essential for coordinating mitochondrial replication and transcription; alterations to this mitochondrial biogenesis network can lead to decreases in mitochondrial density, altered oxidative metabolism and the development of disease such as the insulin resistance and the metabolic syndrome.

Intermembrane Space
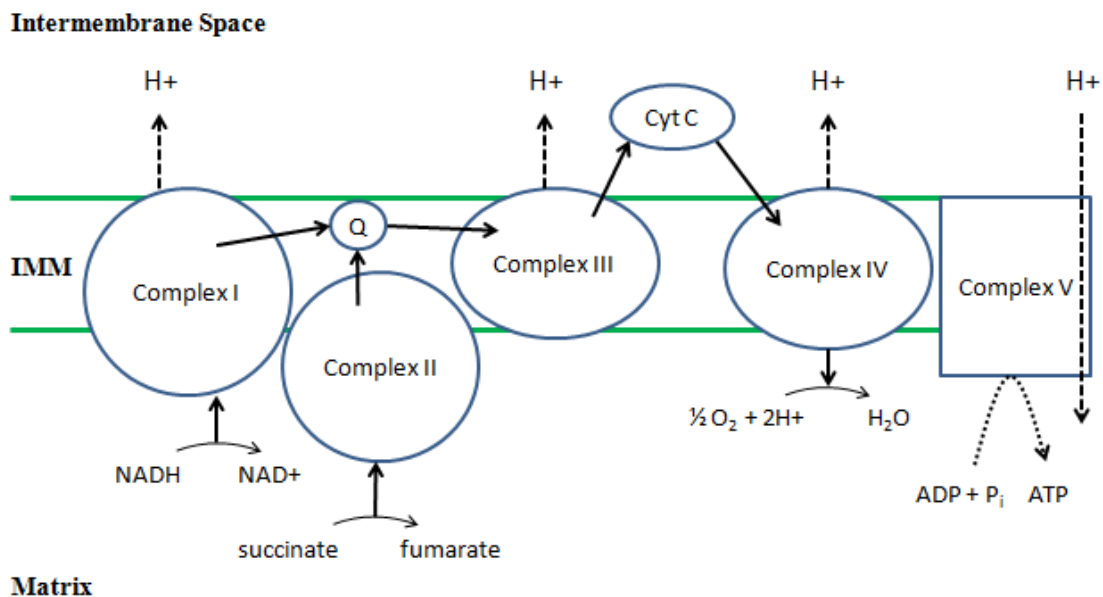
Figure 1.1. Summary of the flow of electrons and protons through the ETC. Depicted are the five complexes embedded in the lipid bilayer of the inner mitochondrial membrane (IMM) and the two dissociable electron carriers, cytochrome C (cyt C) and coenzyme Q (Q). The solid arrows indicate the flow of electrons. The dashed arrows indicate the flow of protons by proton pumping by complex I, III and IV to the intermembrane space and through complex V to the mitochondrial matrix which is coupled with synthesis of ATP.
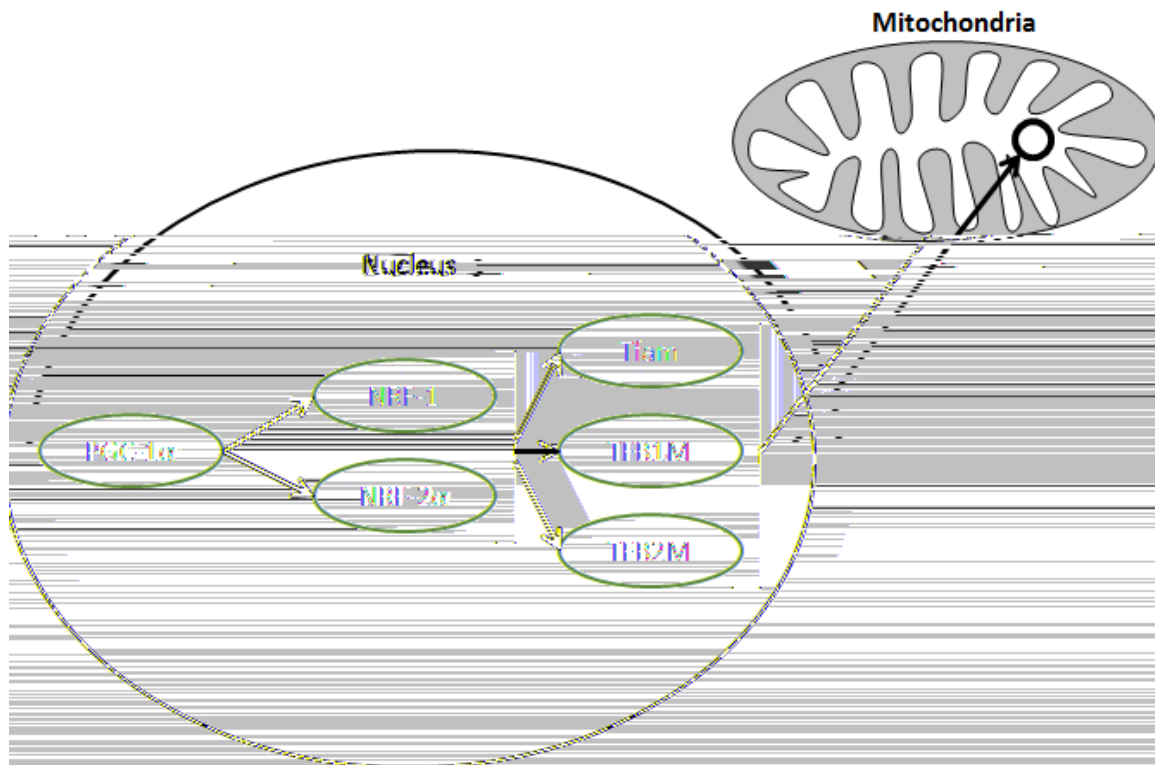
Figure 1.2. The network of co-activators and transcription factors involved in coordinated transcription for mitochondrial biogenesis. PGC-1α and co-activators in the same family, such as PGC-1β, induce expression of the transcription factors NRF-1 and NRF-2α. PGC-1α can also bind with these transcription factors and enhance expression of nuclear-encoded mitochondrial genes. NRF-1 and NRF-2α are also responsible for the expression of the mitochondrial transcription factors Tfam, TFB1M and TFB2M. These three transcription factors translocate to the mitochondria and are essential for transcription and replication of mtDNA (depicted as circle in mitochondria).

1.4 The mitochondria as a source and target of hypoxic signaling

1.4.1 Hypoxic signaling alters oxidative metabolism

HIF-1α is a well-documented regulator of gene expression under hypoxia. Under normoxic conditions, proline residues 564 and 402 of HIF-1α become hydroxylated which leads to ubiquination and degradation (Turrens, 2003). In contrast, under hypoxia HIF-1α is stabilized and initiates expression of genes under the control of the hypoxic response element (Chandel et al. 1998).

One of the important responses HIF-1α induces is a shift from oxidative phosphorylation towards glycolytic metabolism by stimulating the expression of glycolytic enzymes (Seagroves et al., 2008; Papandreou et al. 2006). This is an important contributor to reducing the amount of O_2 that is used in the cell, bypassing OXPHOS, while still maintaining ATP production through glycolysis. Regulating the use of O_2 by suppression of the TCA cycle and OXPHOS helps to maintain cellular ATP and O_2 levels and is suggested to be essential for the survival of hypoxic cells (Papandreou et al., 2006; Kim et al., 2006). Coincident with the depression of mitochondrial OXPHOS under hypoxia there is also an up-regulation of pyruvate dehydrogenase kinase (PDHK). Pyruvate is the last substrate produced in glycolysis and enters the TCA cycle after being converted to acetyl-CoA by pyruvate dehydrogenase (PDH). PDHKs regulate pyruvate entry into the TCA cycle by decreasing PDH activity (Papandreou *et al*., 2006). These hypoxia-induced responses essentially depress mitochondrial function within the cell, indicating the mitochondrion as a main target of hypoxia-induced regulation.

1.4.2 Mitochondrial increase in ROS as an oxygen-sensing mechanism

Recent research has shed light into the response of the mitochondria to decreases in O_2 tension. Studies have utilized the fluorescent probe for intracellular reactive oxygen species (ROS) dichlorofluorescein (DCF) where oxidation of reduced DCF (DCFH) by ROS generates the fluorescent compound DCF (Chandel *et al*., 2000). DCF fluorescence increases after exposure to hypoxia in a variety of cell types such as human hepatoma cells, cardiomyocytes and skeletal muscle (Zuo and Clanton, 2005; Chandel *et al*., 2000; Vanden Hoek et al., 1998). Furthermore, the ETC has been implicated as the source of this ROS as cells with depleted mtDNA or inhibited ETC show no increases in ROS under hypoxia (Schroedl et al., 2002; Chandel et al., 1998; Vanden Hoek et al., 1998).

This seemingly paradoxical increase in ROS has now been implicated as a role in hypoxic signaling in a variety of cell types (Hoppeler et al., 2003; Schroedl et al., 2002; Chandel et al., 1998) including skeletal muscle cells (Brunelle *et al*., 2005). Exogenous supplementation of the cytosol with H_2O_2 stabilized HIF-1α under normoxia (Chandel et al., 2000) and HIF-1α stabilization was inhibited by the over-expression of catalase, an enzyme which converts H_2O_2 to O_2 and H_2O (Hoppeler et al., 2003). The mitochondrion is an essential producer of ROS within the cell during hypoxia, thereby contributing directly to the stabilization of HIF-1α.

1.4.3 ETC as the source of ROS at the onset of hypoxia

The mitochondrion, the main consumer of O_2 within the cell, plays an important role during hypoxia. Although the mitochondrion may be an important producer of ROS under hypoxic stress, the mechanism of hypoxic ROS production is still under debate.

One hypothesis implicates complex IV and nitric oxide (NO) as a possible mechanism of O_2 sensing (Alvarez *et al.* 2002, Cooper and Davies, 2000). NO levels increase by NO synthase under hypoxia. NO can reversibly bind to the oxygen-binding site of cytochrome oxidase effectively increasing the Km of complex IV for O_2 (Cooper and Davies, 2000). This decrease in O_2 affinity at low O_2 concentrations is assumed to cause the upstream ETC complexes to remain reduced; the remaining O_2 is likely to be reduced by these complexes to the superoxide anion (O_2^-). NO can disassociate quickly facilitating a quick recovery of the electron transport chain when re-oxygenated (Cooper and Davies, 2000).

Complex III has been implicated as the main component of the ETC which is required for both increases in ROS under hypoxia and cellular O_2 sensing in cardiomyocytes (Kulisz *et al*., 2002), pulmonary vascular cells (Paddenberg *et al*., 2002) and skeletal muscle (Anderson and Neufer, 2005). Of the three major sources of ROS within the ETC, only Complex III releases ROS into both the intermembrane space and matrix, whereas Complex I and II release all superoxides only to the matrix, which are unlikely to reach the cytosol of the cell. (Bell et al. 2007). A knockdown of complex III activity is associated with inhibition of the stabilization of HIF-1α and decreased ROS production under hypoxia (Guzy *et al.*, 2005).

The ETC is emerging as an important sensor of O_2 within the cell during hypoxic insults. The combined decrease in activity of Complex IV and the implications of Complex III as the main producer of ROS that can easily penetrate the cytosol to stabilize HIF-1α shows the importance of the mitochondria within hypoxic signaling. Increases in ROS, however, can also have damaging effects on the cell. In long-term cases, this increase in ROS must be down-regulated by down-regulating OXPHOS and O_2 consumption.

1.4.4 Hypoxia-induced alterations to metabolism and the mitochondria under prolonged hypoxia

Signaling mechanisms alter the cells so they can survive either an acute or chronic hypoxic insult. Hypoxia-induced signaling cascades under severe hypoxia can lead to genetic instability such as reduced DNA mismatch repair activity and down-regulation of DNA repair genes (Greijer and van der Wall, 2003). Therefore, the first response of the hypoxic cell is to decrease mitochondrial O_2 consumption, an important step for survival to avoid hypoxia-induced apoptosis. A switch to glycolytic metabolism and increases in pyruvate dehydrogenase kinase facilitates this response, however, decreases in mitochondrial OXPHOS may not be solely dependent on alterations to stages of metabolism upstream of the ETC; the ETC and mitochondrial biogenesis may be altered directly.

The initial burst in ROS is acute during the onset of hypoxia, and ROS levels quickly decrease within an hour of continued hypoxia (Chandel et al., 1998). High levels of ROS within the cell can be damaging, therefore, a decrease in ROS may be necessary for continued survival of the cell under hypoxia. An essential response of the cell may be a suppression of the ETC to reduce ROS production. Piruat and Lopez-Barneo (2005) discovered that mRNA of specific subunits of complex I transcribed from mtDNA (ND4 and ND5) were depressed after 24 hours of hypoxia; this depression reached a plateau in some cases as early as 6 hours under hypoxia (Piruat and Lopez-Barneo, 2005). This effect has also been observed in rat cardiac cells, where complex I protein levels were depressed after a hypoxic insult (Heather *et al*., 2012). These alterations in complex I protein coincided with decreased complex I enzymatic activity (Heather *et al*., 2012; Piruat and Barneo, 2005). Impaired enzymatic activity of complexes II and IV (Heather *et*

al., 2012) and reduced O_2 consumption linked to decreased ETC activity have also been observed (Papandreou *et al*., 2006). These findings highlight O_2 levels as a major contributor to physiological alterations to the mitochondrial ETC and ultimately O_2 consumption.

1.5 Resveratrol, a pharmacological intervention for mitochondrial dysfunction in skeletal muscle

Compromised mitochondrial function is associated with a variety of conditions including metabolic and cardiovascular disease (Lagouge *et al*., 2006). Type 2 diabetic patients have decreases in mitochondrial biogenesis and reduced levels of mitochondrial transcription factors and co-activators (Lagouge *et al.*, 2006; Mootha *et al*., 2004; Patti *et al*., 2003). Therefore, pharmacological interventions that promote mitochondrial density and function are ideal targets for diabetic patients. One of the most popular interventions in current research is resveratrol (RSV).

RSV is a polyphenolic compound which is most commonly found in the skin of red grapes, as well as other plant-based dietary and herbal sources (Park *et al*., 2012; Lagouge *et al*., 2006; Baur and Sinclair, 2006). RSV has global effects such as anti-inflammatory, anti-carcinogenic and antioxidant activity (Baur and Sinclair, 2006). Most important in terms of mitochondrial dysfunction diseases, RSV up-regulates mitochondrial biogenesis by increasing the activity of the Sirtuin-1 (SIRT1) and PGC-1α pathway. SIRT1 is an NAD+ dependant deacetylase which activates PGC-1α (Baur and Sinclair, 2006), an important co-factor in the regulation of mitochondrial biogenesis. Therefore, RSV treatment may increase mitochondrial biogenesis and skeletal muscle oxidative capacity mediated by PGC-1α and SIRT1.

RSV inhibits phoshpodiesterase (PDE) hydrolysis of cAMP to 5'-AMP (Park *et al*., 2012). The resulting increase in cellular cAMP levels leads to an increase in cAMP binding to Epac1 (a cAMP effector protein) which increases calcium ion levels by inducing phosphorylation of ryanodine receptor 2 (Ryr2), a calcium channel (Figure 1.3). This calcium signaling activates AMP-activated protein kinase (AMPK) which increases NAD+ levels and, thereby increasing SIRT1 activity (Park *et al*., 2012; Figure 1.3). AMPK is a conserved 'fuel sensor', which is critical for mitochondrial biogenesis in muscle tissue under chronic energy deprivation (Zong *et al*., 2002; Bergeron *et al*., 2001). Ultimately, inhibition of PDE and the subsequent signaling pathway lead to an increase in PGC-1α, PGC-1β, NRF1 and Tfam expression (Park *et al*., 2012; Timmers *et al*., 2011). Although RSV is also considered to activate other signaling pathways, such as those involving estrogen and thyroid hormone, in skeletal muscle RSV increases only the SIRT1 pathway (Lagouge *et al*., 2006). The targeted increases in mitochondrial biogenesis by RSV may be an important intervention in skeletal muscle with a low density of mitochondria that are inherently dysfunctional, such as skeletal muscle exposed to chronic hypoxia during development.

1.6 Thesis Objectives

Hypoxia *in utero* has negative effects on fetal development, and these effects are thought to persist after birth. Specifically, hypoxia *in utero* is thought to impact skeletal muscle mitochondrial biogenesis and metabolism pre-disposing offspring to metabolic diseases, such as insulin resistance, in adult life. I hypothesize that skeletal muscle development under hypoxia will have significant effects on mitochondrial oxidative

metabolism, mitochondrial biogenesis and the ETC. Furthermore, I hypothesize that these alterations will persist following a recovery under normoxic conditions. Finally, I hypothesize that RSV, a promoter of mitochondrial biogenesis, will reverse these alterations.

Prediction One

Skeletal muscle cells that differentiate under hypoxia will have reduced rates of O_2 consumption in conjunction with altered markers of mitochondrial biogenesis and decreases in the protein levels of the electron transport chain complexes. I predict that these alterations will persist following a recovery under normoxia.

Prediction Two

RSV will reverse the depressed O_2 consumption rates and increase expression of markers of mitochondrial biogenesis.
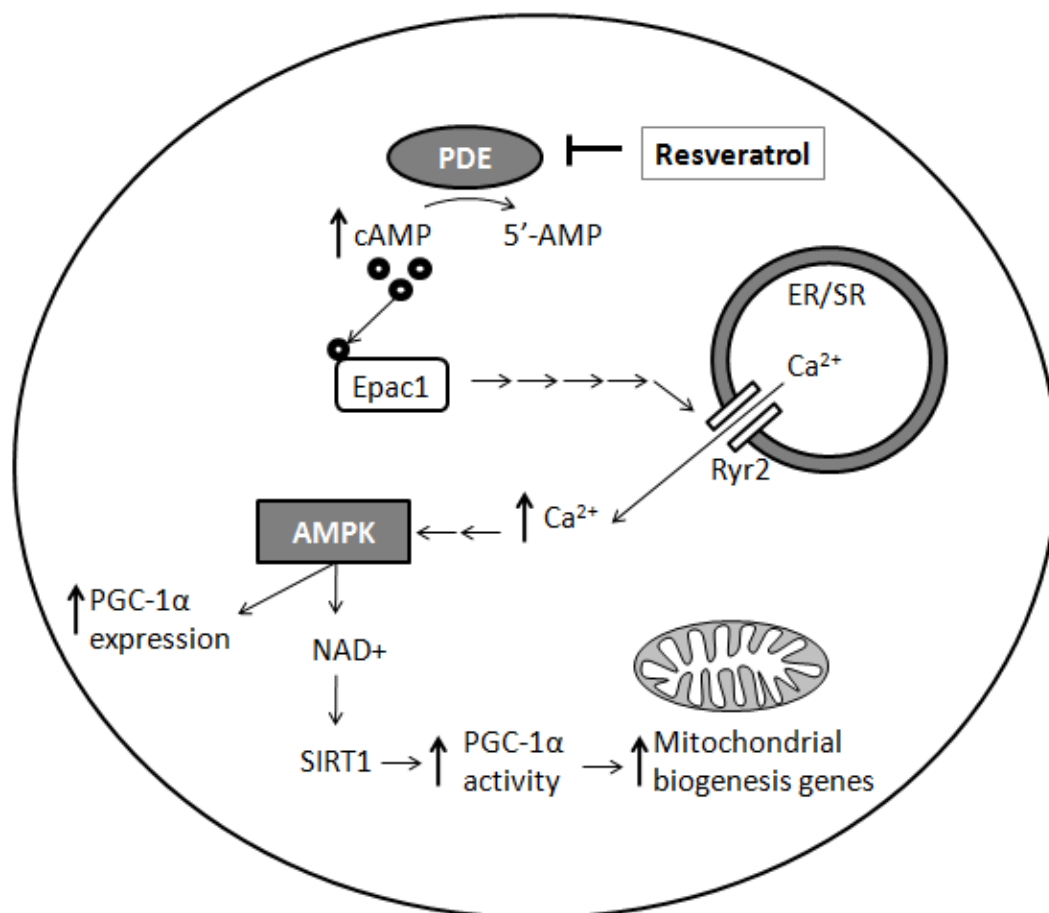
Figure 1.3. Model of how RSV acts within the cell to increase mitochondrial biogenesis. Figure adapted from Park *et al*., 2012. Resveratrol inhibits PDE which subsequently increases cAMP levels. This increase in cAMP leads to an increased activation of Epac1, and after a series of steps activates Ryr2 (calcium channel depicted on endoplasmic reticulum/smooth endoplasmic reticulum; ER/SR). Activation of this channel leads to an increase in calcium ions within the cytosol, eventually leading to an increased activation of AMPK. Finally AMPK is responsible for inducing PGC-1α expression and increasing NAD+ levels to activate SIRT1. These responses ultimately cause an increase in PGC-1α activity which induces expression of mitochondrial biogenesis genes.

Chapter 2: Materials and Methods

2.1 *In vitro* model of hypoxia

2.1.1 The C_2C_{12} mouse muscle myoblast cell line

The mouse C_2C_{12} myoblast cell line (ATCC, catalogue number CRL-1772, Manassas, VA) was used in this study as a model of skeletal muscle differentiation under hypoxia. The C_2C_{12} cell line is derived from myoblast satellite cells and has been extensively used in hypoxic studies (Yun *et al.* 2005; Arthur *et al.* 2000). Differentiation from myoblasts to myotubes can be readily induced in C_2C_{12} cells, a process that closely recapitulates fetal muscle development making it ideal for my study (Messina *et al.*, 2010; Biressi *et al.* 2007). Although these are adult derived cells, C_2C_{12} cells have been shown to be an effective model for fetal skeletal muscle development as important structural and differentiation markers are all found in C_2C_{12} myotubes *in vitro*, which closely parallels *in vivo* muscle development and growth. (Burattini *et al.*, 2004)

Myoblast cells were maintained at 37°C in a growth media of Dulbecco's Modified Eagle's Medium (DMEM) supplemented with 10% fetal bovine serum (FBS) and 1% penicillin/streptomycin for 48 hours (approximately 80% confluency on the plate) at 20.9% oxygen (5% CO_2 with nitrogen [N_2] balance). After 48 hours, growth medium was replaced with differentiation medium (DMEM supplemented with 5% horse serum (HS) and 1% penicillin/streptomycin) to induce differentiation from myoblasts to myotubes. The cells were incubated at 37°C at 1% (approximating IUGR hypoxia; Regnault *et al.*, 2007), 5% (fetal normoxia; Regnault *et al.*, 2007) or 20.9% (air saturation frequently used in cell culture studies) O_2 for five days of differentiation. Another subset

of cells from each treatment was incubated at 20.9% O_2 for an additional two days to evaluate potential recovery from the hypoxic insult (Figure 2.1).

2.1.2 RSV as a pharmacological intervention during recovery

The C_2C_{12} myoblast cell line was cultured as described in section 2.1.1 for the initial five days of differentiation, however, at Day 5, a subset of cells from each of the three O_2 treatments was prepared for recovery by treatment with RSV (50 µM) or DMSO (5.63 µM; the vehicle resveratrol is dissolved in) media and incubated at 20.9% oxygen for an additional two days (Day 7, recovery; Figure 2.2). The concentration of resveratrol chosen for these experiments corresponds to concentrations previously used with the C_2C_{12} mouse muscle myoblast cell line (Park *et al*., 2012) and is within the range of plasma levels reported *in vivo* when resveratrol is administered at pharmacologically relevant levels in rodent models (Lagouge *et al*., 2006; Baur and Sinclair, 2006).

2.2 Cell sampling

C_2C_{12} cells were collected, as outlined in Figure 2.1 and 2.2, at various time-points through the experiment: Day 0 (cells grown at 20.9% O_2 before growth medium was replaced with differentiation medium), Day 5 (cells after five days of differentiation under one of three O_2 treatments) and Recovery (cells after Day 5 and the two day recovery period at 20.9% oxygen with medium that was untreated, treated with DMSO or treated with resveratrol).
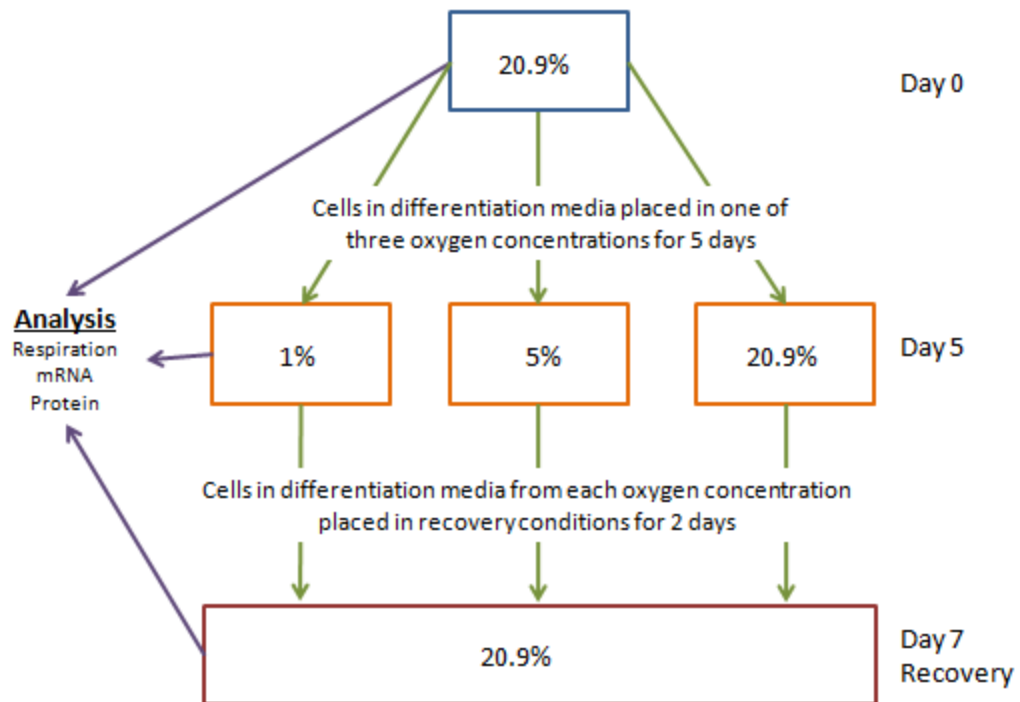
Figure 2.1. Schematic of cell culture procedures and sampling. Following attainment of approximately 80% confluency in growth medium (Day 0), C_2C_{12} mouse muscle myoblasts were differentiated under 1%, 5% or 20.9% O_2 for five days (Day 5). A subset of cells from each O_2 concentration was placed in a recovery condition of 20.9% O_2 for an additional two days (Day 7).
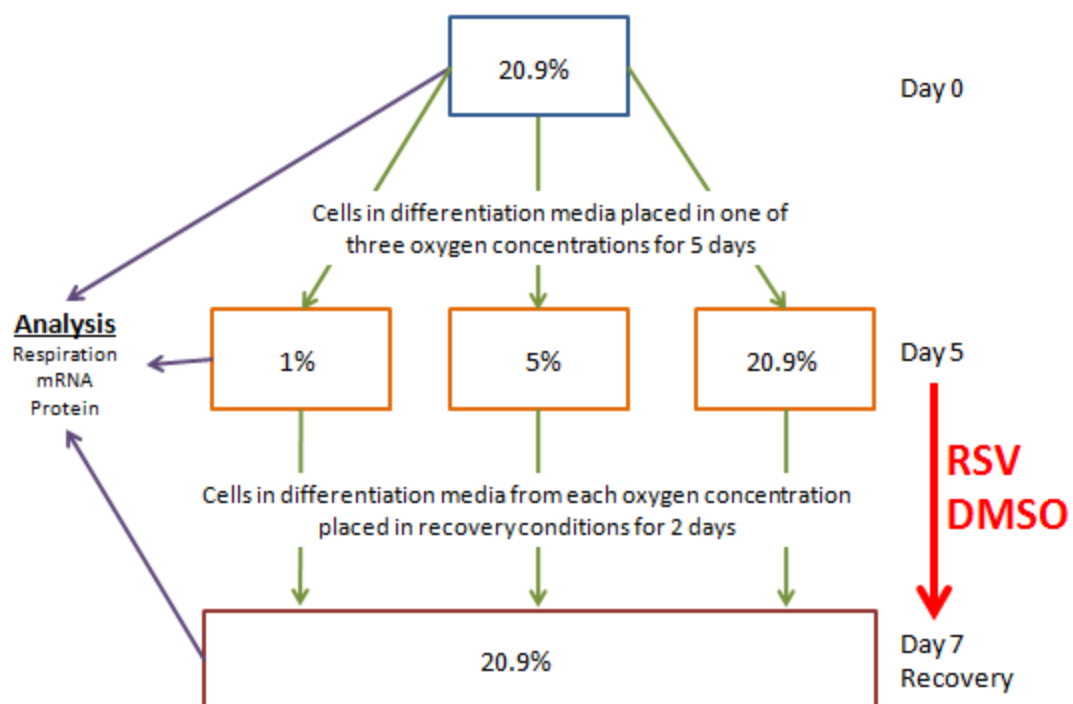
Figure 2.2. Schematic of cell culture procedures and sampling for DMSO and RSV treated cells. Following attainment of approximately 80% confluency in growth medium (Day 0), C_2C_{12} mouse muscle myoblasts were differentiated under 1%, 5% or 20.9% O_2 for five days (Day 5). A subset of cells from each O_2 concentration was incubated in a recovery condition of 20.9% O_2 for an additional two days (Day 7). During the recovery period, cells were treated with differentiation medium supplemented with either 50 µM RSV or its vehicle DMSO (4 µl/10 ml of media).

2.3 Oxygen Consumption Rate

2.3.1 Cells with untreated media during recovery

Whole cell respiration analysis of the C_2C_{12} cells was evaluated using the Oxygraph-2k (Oroboros instruments, Innsbruck, Austria). Cells were released from the plate using trypsin, centrifuged at 1000 x g and re-suspended in cell buffer (25 mM HEPES, 130 mM NaCl, 5 mM KCl, 0.5 mM $MgCl_2$ [pH 7.4] with 10 mM glucose as oxidative substrate). Oxygen consumption was measured at 37°C using Clark-type oxygen electrodes in an airtight chamber with stirring at 750 RPM. Cellular respiration resulted in a decline in dissolved O_2 concentration within the chambers, and O_2 consumption rates were calculated by the Datlab software (Oroboros Instruments) from this decline. These rates were reported at dissolved O_2 concentrations of 200 μM, 50 μM and 10 μM, which approximate the 1%, 5% and 20.9% gaseous O_2 condition respectively, under which the cells differentiated. Oxygen consumption rates were expressed per 10^6 viable cells with cell density determined using a haemocytometer. The viability of cells was assessed using trypan blue which stains dead cells blue as previously described in Yun *et al*. (2005).

2.3.2 Cells with RSV or DMSO treated media during recovery

Whole cell respiration was evaluated at O_2 concentrations calculated to be similar to those used in this study; 200 μM, 50 μM and 10 μM of O_2 within the chamber which approximate the 1%, 5% and 20.9% gaseous O_2 condition, respectively, under which the cells differentiated. Nitrogen was used to displace the oxygen within the airtight Oxygraph-2k chamber. After the oxygen consumption rate had reached a steady state at

200 μM, the chamber lid was raised slightly and 1 to 2 ml N_2 gas was introduced to the gas space above the cell buffer in the chamber to displace the oxygen to the desired O_2 concentration; the lid was then replaced and secured making the chamber airtight and again allowed to reach a steady O_2 consumption rate. This N_2 technique allowed for more rapid determination of O_2 consumption rates. Day 5 measurements with this technique produced similar patterns of O_2 consumption compared with data collected in section 2.3.1.

2.4 Molecular analysis

2.4.1 Quantitative real-time PCR analysis of mRNA

Cell samples were collected in Trizol reagent (Invitrogen, Carlsbad, CA) and stored at -80°C until use for RNA isolation. Total RNA was isolated from C_2C_{12} cells using a Trizol reagent isolation procedure. Samples were thawed, and incubated in Trizol at room temperature for 5 minutes. For every milliliter of Trizol used initially, 200μl of chloroform were added to the solution, shaken vigorously by hand for 15 minutes and left at room temperature for 3 minutes. Samples were then centrifuged for 15 minutes at 12,000 x g at 4°C to separate the RNA in the chloroform top phase from the waste products in the lower Trizol layer. The top chloroform phase was removed and placed in a fresh tube and 500μl of isopropyl alcohol were added to the top phase for every milliliter of Trizol used initially. This mixture was incubated at room temperature for 10 minutes then centrifuged at 12,000 x g for 15 minutes at 4°C. The chloroform and isopropyl alcohol supernatant was poured off, and the pellet was washed twice by adding 200 μl of 75% ethanol without re-suspending the pellet and spun at 12,000 x g for 5 minutes at 4°C.

The ethanol was removed with a pipette. These pellets were dissolved in diethylpyrocarbonate treated water for 5 minutes at room temperature and stored in -80°C until use for cDNA generation.

The yield of isolated RNA was determined using a NanoDrop 2000 spectrophotometer (Thermo-Scientific) and quality was measured using the A260/A280 ratio (≥1.8). To further ensure RNA quality, samples were seperated on a 1.2% agarose gel containing ethidium bromide. Samples were screened for degradation by the visualization of the 28S:18S bands; only samples without degradation were used for further analysis.

Isolated RNA (5 μg) was incubated with deoxyribonuclease (Invitrogen) to remove any contaminating DNA and a recombinant ribonuclease inhibitor (Invitrogen) at 37°C for 30 minutes. Samples were then incubated at 37°C for two hours with murine leukemia virus reverse transcriptase (Invitrogen) to produce cDNA with the use of random primers.

Real-time quantitative PCR (qPCR) was performed using SsoFast EvaGreen Supermix (Invitrogen) and the BioRad CFX384 Real-Time PCR Detection System. A total volume of 8 μl in each well contained 60 ng of cDNA (3 μl), 0.08 μl primer mix, 4ul SYBR Green and the remaining volume was filled with autoclaved water. Primers sets for *NRF-1*, *NRF-2α*, *Tfam*, *TFB1M* and *TFB2M* were adapted from Liu and Brooks (2011). Primer sets directed against mouse-specific *PGC-1α* and *β* were generated using the NCBI Primer-BLAST tool based on published *Mus musculus* sequences (Table 2.1). The data from qPCR was analyzed using the $2^{-\Delta\Delta Ct}$ method (Livak and Schmittgen, 2001) using ribosomal protein 7 (RL7) as the internal control gene.

Table 2.1. Primer sequences for qPCR.

Primers	Target Length/ NCBI Accession #	Strand	Sequence (5'→ 3')
NRF-1	255 b.p. NM_001164226.1	Forward Reverse	TCTCACCCTCCAAACCCAAC CCCGACCTGTGGAATACTTG
NRF-2α	129 b.p. NM_008065.2	Forward Reverse	CTCCCGCTACACCGACTAC TCTGACCATTGTTTCCTGTTCTG
Tfam	172 b.p. NM_009360.4	Forward Reverse	CATTTATGTATCTGAAAGCTTCC CTCTTCCCAAGACTTCATTTC
TFB1M	102 b.p. NM_146074.1	Forward Reverse	AAGATGGCCCTTTCGTTTATGG GACTGTGCTGTTTGCTTCCTG
TFB2M	135 b.p. NM_008249.4	Forward Reverse	CCAAAACCCATCCCGTCCAAAT AAGGGCTCCAAATGTGGAATAAA
PGC-1β	112 b.p. NM_133249.2	Forward Reverse	CCCTCTGCCAACGGAAACAA TGTGAGACTGGCACGGATCT
PGC-1α	161 b.p. NM_008904.2	Forward Reverse	AACGATGACCCTCCTCACAC GGGTCATTTGGTGACTCTGG
RL7	202 b.p. NM_011291.5	Forward Reverse	GGAGCTCATCTATGAGAAGGC AAGACGAAGGAGCTGCAGAAC

2.4.2 Mitochondrial protein extraction

C_2C_{12} myoblasts and myotubes were collected in a phosphate buffer saline (D-PBS) solution supplemented with a 10X protease/phosphatase inhibitor (Thermo Scientific Halt protease/phosphatise inhibitor 100X solution, catalogue number 7446; Rockford, IL). Suspended cells were centrifuged at 1000 x g for 5 minutes to form a pellet. A mannitol-based solution (0.3 M Mannitol, 0.1% BSA, 0.2mM EDTA, 10mM HEPES, adjusted to a pH of 7.4 with KOH) was used to isolate crude mitochondria from the pelleted cells. The mitochondrial isolation buffer was supplemented with a 10X protease/phosphatase inhibitor on the day of collection. Pelleted cells were re-suspended in 500 µl of cold isolation buffer. Cells were then sonicated for four seconds at 20 Amp to disrupt the cell membranes. Samples were then centrifuged at 1000 x g for 10 minutes at $4^{o}C$. The supernatant was collected and the pellet, containing whole cells and nuclei, was discarded. The supernatant was then centrifuged at 14,000 x g for 15 minutes at $4^{o}C$. The pellet containing the mitochondrial fraction was washed twice by adding 100 µl of cold isolation buffer and centrifuging at 14,000 x g for 1 minute. The isolation buffer was removed with a pipette and the pellet was stored at $-20^{o}C$ until the protein concentration could be assessed.

2.4.3 Protein quantification and Western blotting

The pelleted mitochondria were solubilized in D-PBS supplemented with 1% Sodium dodecyl sulfate, a detergent. Protein concentration was evaluated using the *DC* Protein Assay Kit (BioRad). Samples were then prepared using NuPAGE LDS sample buffer (Invitrogen) and NuPAGE Sample Reducing Agent (Invitrogen). Approximately

12µg of mitochondrial extracts were seperated on NuPAGE 4-12% Bis-Tris gels (Invitrogen) in MES-SDS running buffer at 200V for 1 hour. After transfer to nitrocellulose membranes (100V, 2 hours), membranes were blocked for one hour in 5% milk in D-PBS then subsequently washed three times with 1% Tween in D-PBS for 10 minutes. Membranes were then incubated overnight at 4°C in 1% milk in D-PBS supplemented with the MitoProfile Total OXPHOS Rodent Antibody Cocktail (Complex I subunit NADH dehydrogenase [ubiquinone] 1 beta subcomplex 8, NDUFB8; Complex II Iron-sulfur protein subunit; Complex III Core protein 2; Complex IV subunit I; Complex V alpha subunit) at a 1:1000 dilution (ab110413, host: mouse; Mitosciences, Eugene, OR). Membranes were then washed three times with 1% Tween in D-PBS for 10 minutes and then incubated for one hour at room temperature in 1% milk in D-PBS supplemented with a donkey anti-mouse horseradish peroxidase secondary antibody. To probe for the housekeeping protein (voltage dependent anion-selective channel protein 1, VDAC1), membranes were prepared in a similar manner as described above with primary antibody at a 1:1000 dilution (ab14734, host: mouse; Invitrogen). Immunoreactive bands were detected with enhanced chemiluminescence and imaged with a VersaDoc Imaging System (Bio-Rad, Richmond, CA). Densitometry was performed with Quantity One Software (Bio-Rad).

2.5 Flow cytometry

Flow cytometry was employed to determine fluorescence of probes used to assess levels of ROS and mitochondrial abundance. DCF (C6827, Invitrogen) was used to determine the relative amounts of ROS within the entire live cell as this probe fluoresces

green when oxidized by a variety of ROS. MitoSOX Red mitochondrial superoxide indicator (MS36008, Invitrogen) specifically targets mitochondria after permeating live cells and fluoresces red when oxidized by superoxides. These probes were validated previously by performing positive control experiments with the application of hydrogen peroxide to C_2C_{12} cells to induce ROS formation. Mitotracker Red CMXRos (M7512, Invitrogen) permeates live cells and labels mitochondria; the probe accumulates according to the membrane potential of the mitochondrion and fluoresces red. After incubation, control (without fluorescent probe) and treated (with fluorescent probe; table 2.2) cell samples were run through the BD Accuri C6 flow cytometer equipped with a blue and red laser (excitation), two light scatter detectors, and four different colour fluorescence detectors (emission detection; 533/30 nm, 585/40 nm, > 670 nm, 675/25 nm). Mean fluorescence was subsequently calculated by the BD CFlow software. The background mean fluorescence of the control sample was subtracted from the mean fluorescence of the treated samples.

2.6 Citrate synthase activity assay

Citrate synthase (CS) was assayed to estimate mitochondrial abundance. Cells were collected as described in section 2.3.1, and 500 µl were stored at -80°C until ready for analysis. Cells suspended in cell buffer were sonicated to disrupt cell membranes and kept on ice until ready to be loaded on a 96-well plate. Reagents for the CS assay were prepared as outlined in Table 2.3. Spectrophotometer temperature was set to 37°C. A 96-well plate was prepared with control and experimental wells for each sample in triplicate. Control wells contained 220 µl of CS buffer, 30 µl of 5,5'-dithio-bis(2-nitrobenzoic acid)

(DTNB), 30µl of acetyl CoA and 20 µl of sample. Experimental wells contained the same as control wells except for the addition of 3 µl of oxaloacetate. Absorbance of the wells was immediately read at 412nm for 5 minutes under kinetic settings and maximal activity was calculated based on a minimum of 9 consecutive readings during the 5 minutes. Further calculations corrected for the path length, extinction coefficient, number of viable cells per sample and background absorbance as determined by the control. Data was expressed as enzymatic activity (arbitrary unit).

2.7 Statistical analysis

All data is presented as mean ± SEM. All data were analyzed with a Two-way ANOVA using SigmaPlot 12 software to compare the day or treatment with the O_2 concentration during differentiation. Significance was set at a P-value of 0.05 or less, and a Tukey's post-hoc test was performed on statistically significant data. Any set of data that failed the Shapiro-Wilk normality test or equal variance test (F-test) were transformed using the $\log_{10}$ or square root transformation and re-tested for normality and equal variance.

Table 2.2. Incubation procedures and excitation/emission for specific probes in flow cytometry to quantify levels of ROS and relative mitochondrial abundance.

Probe	Incubation	Excitation	Emission
Mitotracker	Differentiation or growth medium supplemented with Mitotracker (250 nM) for 20 minutes	579 nm	599 nm
MitoSOX	Hank's balanced salt solution supplemented with MitoSOX (5μM) for 15 minutes	510 nm	580 nm
DCF	Hank's balanced salt solution supplemented with (5 μM) DCF for 30 minutes	492 - 495 nm	517 - 527 nm

Table 2.3. Reagent preparation for CS assay.

Reagent	Concentration in well	Preparation
CS buffer	50 mM	0.185 g Trizma base in 50 ml water pH 8.0 at 37°C
Acetyl CoA	0.15 mM	0.0012 g to 1 ml of CS buffer
DTNB	0.15 mM	0.0006 g to 1 ml of CS buffer
Oxaloacetate	0.33 mM	0.0044 g to 1 ml of CS buffer

Chapter 3: Results

3.1 Hypoxia-induced alterations to mitochondrial function in skeletal muscle cells

3.1.1 Hypoxia depresses the oxygen consumption rate in C_2C_{12} skeletal muscle cells

In order to verify that differentiation under hypoxia alters oxidative metabolism, the oxygen consumption rate of C_2C_{12} mouse muscle myotubes was determined using an Oxygraph-2k. These myotubes were allowed to respire at their basal metabolic rate until the oxygen in the chamber was depleted. The data from O_2 concentrations of 200 µM, 50 µM and 10 µM within the airtight Oxygraph chamber were analyzed. These dissolved O_2 concentrations represent approximately the 20.9%, 5% and 1% O_2.

Following five days of differentiation, hypoxia significantly reduced oxygen consumption rates at 200 µM. The rate of the 1% O_2 treatment was significantly lower than the 20.9% O_2 treatment ($p < 0.001$) and the 5% O_2 treatment ($p < 0.01$) by 65% and 49%, respectively (Figure 3.1 A). This significant reduction was maintained when O_2 consumption was calculated at 50 µM O_2 with 1% O_2 treatment having rates that were 63% and 57% lower than the 20.9% ($p < 0.01$) and 5% ($p < 0.05$) O_2 treatments, respectively (Figure 3.1 B). This pattern was not maintained when O_2 consumption was calculated at 10 µM O_2 as none of the rates differed significantly ($p > 0.05$; Figure 3.1 C).

Two days of recovery at normoxia did not reverse the hypoxic effect on cellular O_2 consumption rates when measured at 200 µM, 50 µM or 10 µM O_2. At 200 µM, the 1% treatment had a significantly lower oxygen consumption rate than both the 20.9% treatment ($p < 0.001$) and the 5% treatment ($p < 0.01$) by 63% and 48%, respectively

(Figure 3.1 A). This significant reduction was maintained at lower O_2 concentrations within the chamber. At 50 μM the 1% treatment had a 75% lower oxygen consumption rate than 20.9% (p<0.001) and 63% lower than 5% (p<0.01; Figure 3.1 B). Finally, at 10 μM, the 1% treatment had a 76% lower O_2 consumption rate than the 20.9% treatment (p<0.001) and 63% lower than the 5% treatment (p<0.05; Figure 3.1 C). In addition, the 20.9% oxygen treatment had a significant 42% rise in the O_2 consumption rate after recovery at 10 μM (Figure 3.1 C). No significant differences were found between the 20.9% and 5% O_2 treatments at either Day 5 or recovery at all O_2 concentrations analyzed (p>0.05).

3.1.2 Hypoxia did not affect cell viability

The number of viable cells determined using trypan blue staining did not differ among oxygen treatments after either five days of differentiation or subsequent recovery at 20.9% O_2 (p>0.05; Figure 3.2 A).

3.1.3 Mitochondrial abundance is not significantly affected by hypoxia

I used CS activity as one estimate of mitochondrial abundance. No significant differences were observed following five days of differentiation and recovery (p>0.05; Figure 3.2 B) indicating hypoxia does not affect mitochondrial abundance.

Mitochondrial abundance relative to Day 0 (myoblasts before differentiation) was also determined using the mitochondria-specific fluorescent probe, mitotracker. No significant difference was found after five days of differentiation or normoxic recovery

(p>0.05; Figure 3.2 C) further confirming mitochondrial abundance is not affected by differentiation under hypoxia.

3.1.4 Chronic hypoxia does not impact ROS levels

Relative levels of ROS were determined by flow cytometry using fluorescent probes within the whole cell (DCF; Figure 3.3 A) and within the mitochondria (MitoSOX; Figure 3.3 B). Levels of ROS were not affected after five days of differentiation and after two days of recovery at 20.9% O_2 as no significant differences were found (p>0.05; Figure 3.3 A, B).

3.2 Hypoxia-induced alterations to skeletal muscle mRNA and protein

3.2.1 Hypoxia decreases protein levels of a Complex I subunit, NDUFB8

Protein levels of NDUFB8, a nuclear encoded subunit of ETC complex I, were determined in isolated mitochondria and expressed relative to VDAC1, an outer membrane mitochondrial protein. Differentiation under hypoxia (1% O_2) significantly reduced the NDUFB8 protein levels by 64% when compared to the 20.9% O_2 treatment (p<0.05; Figure 3.4). No significant differences were found among the differentiation O_2 groups following normoxic recovery (p>0.05). Furthermore, no changes in the other subunits of the ETC complexes II − V were observed after both hypoxia and recovery (data not shown).

A. 200 μM Oxygen

B. 50 μM Oxygen

C. 10 μM Oxygen
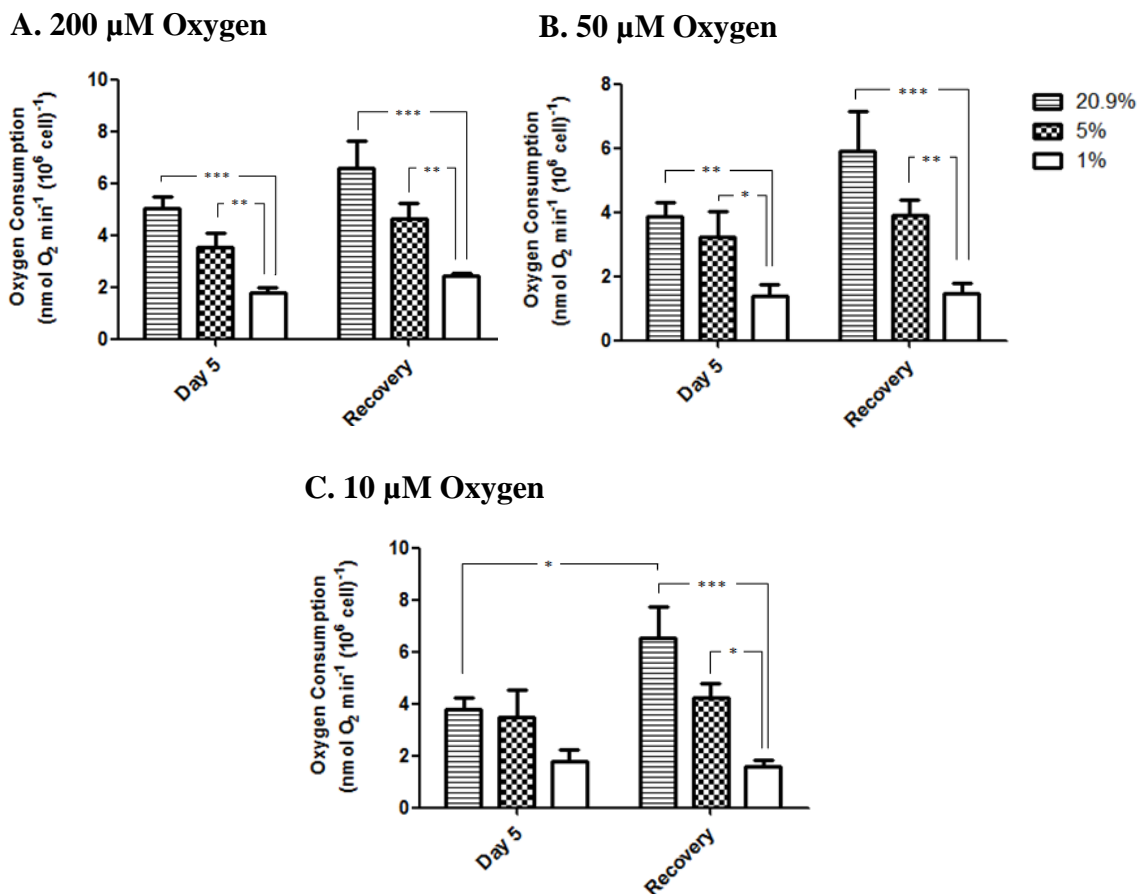
Figure 3.1. Oxygen consumption rates of skeletal muscle cells following differentiation under hypoxia and recovery at normoxia are depressed at varying oxygen concentrations. Oxygen consumption rates were measured by closed-cell respirometry using an Oxygraph-2k Clark-type electrode at 37°C in a 10 mM glucose solution. Data displayed for chamber O_2 concentrations of (A) 200 μM (approximately 20.9% O_2), (B) 50 μM (approximately 5% O_2) and (C) 10 μM (approximately 1% O_2). All data presented as mean ± SEM. Connecting lines indicate a significant difference between those values as determined by a two-way ANOVA with a Tukey's post-hoc test (* $p<0.05$; ** $p<0.01$; *** $p<0.001$; n = 6 – 7/experimental group).
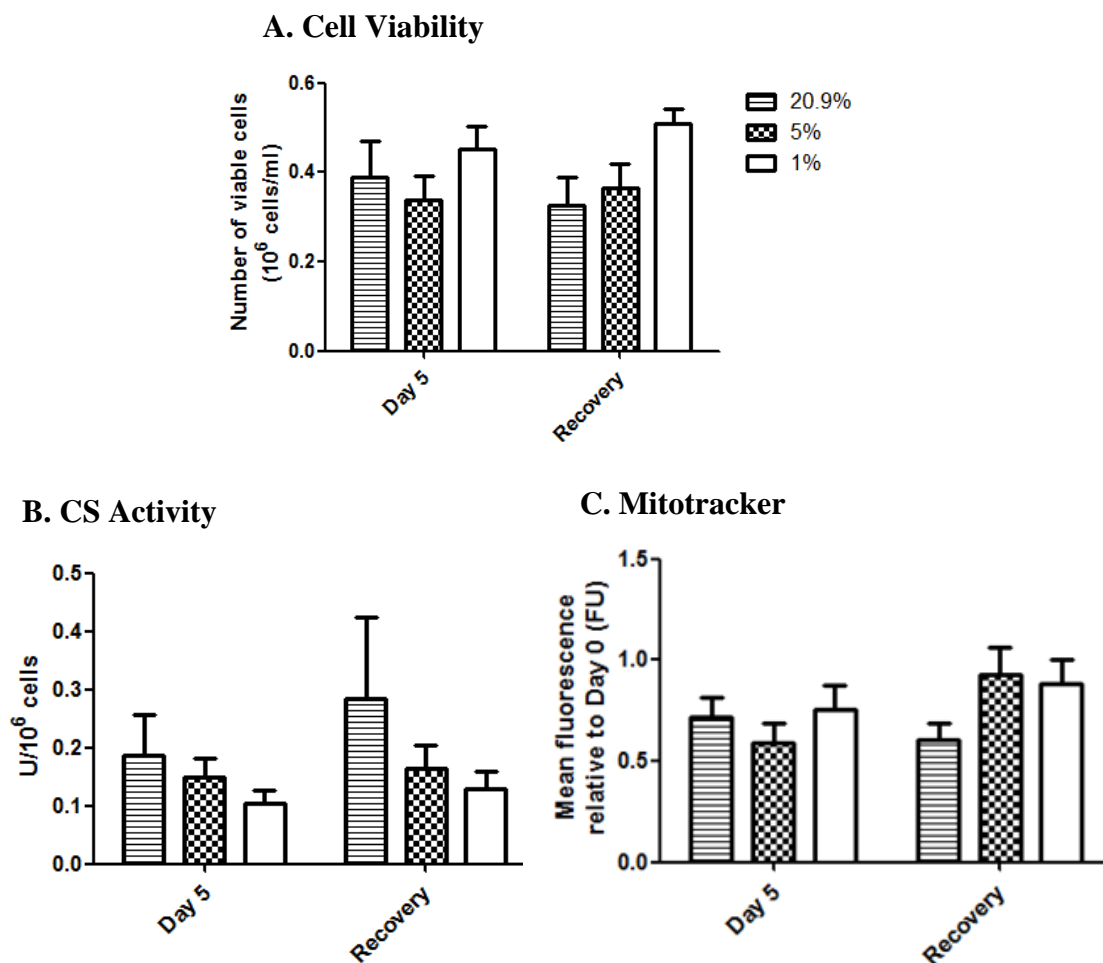
Figure 3.2. The number of viable cells and mitochondrial abundance were not affected by hypoxia. Cell viability was analyzed using a haemocytometer and a trypan blue stain (A; n = 6 - 8/experimental group), no significant differences were found (p>0.05). Mitochondrial abundance was assessed using a CS activity assay (B; n = 3 – 6/experimental group), no significant differences were found (p>0.05). Mitochondrial abundance was further analyzed using flow cytometry and the fluorescent probe Mitotracker and set relative to Day 0 (C; n = 3 – 12/experimental group), no significant differences were observed (p>0.05). All data presented as mean ± SEM and analyzed with a two-way ANOVA.

A. DCF

B. MitoSOX
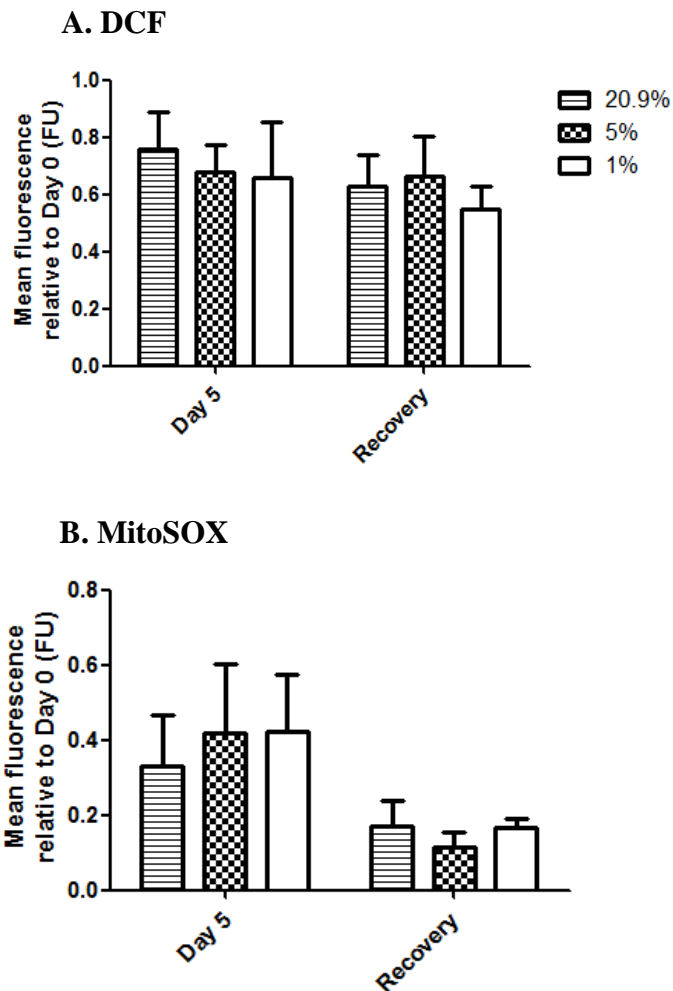
Figure 3.3. Whole cell and mitochondrial ROS are not affected by hypoxia after five days of differentiation and two days of normoxic recovery. Levels of ROS were determined by flow cytometry using the fluorescent probes DCF (A) for whole cell ROS, and MitoSOX (B) for mitochondrial ROS, and are expressed relative to Day 0 (myoblasts before differentiation) levels. No significant difference was found after five days of differentiation under 20.9%, 5% or 1% oxygen or after a two day normoxic recovery period ($p > 0.05$; two-way ANOVA; n = 3/experimental group). All data presented as mean ± SEM.
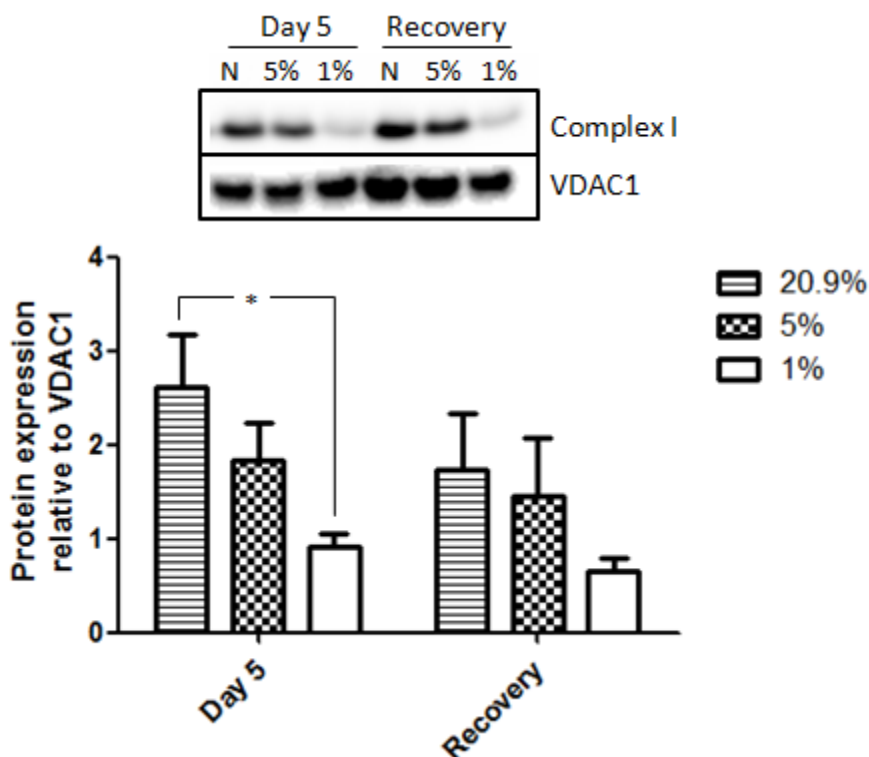
Figure 3.4. NDUFB8, a subunit of ETC complex I, protein levels after five days of differentiation under hypoxia and normoxic recovery. Complex I protein levels were analyzed by Western blot analysis with the antibody for NDUFB8, a nuclear encoded subunit of the ETC Complex I. These levels were standardized to VDAC1, an outer mitochondrial membrane protein expressed at steady state levels as a mitochondrial loading control. Representative blots for NDUFB8 and VDAC1 are displayed above the graph. A two-way ANOVA and Tukey's post-hoc test determined a significant reduction of the 1% treatment protein levels when compared to the 20.9% oxygen treatment at Day 5 (* $p<0.05$; n = 6 – 9/experimental group). All data presented as mean ± SEM.

3.2.2 Expression of some mitochondrial biogenesis transcription factors is affected by hypoxia

The mRNA levels of mitochondrial biogenesis transcription factors were determined by qRT-PCR. *Tfam*, *TFB1M*, and *NRF-1* mRNA levels were unaltered after five days of differentiation under different O_2 levels and recovery at 20.9% O_2 ($p > 0.05$; Figure 3.5 A, B, C). The mRNA levels of *NRF-2α* increased significantly between Day 5 and recovery within the 20.9% and the 1% O_2 treatments by 50% and 42%, respectively ($p < 0.05$; Figure 3.5 D). There was a significant 41% decrease in *TFB2M* mRNA levels of the 1% O_2 treatment following 5 days of differentiation when compared to the 5% O_2 treatment ($p < 0.05$; Figure 3.5 E). A trend towards down-regulation of *TFB1M* mRNA levels was also observed between the 1% and 20.9% O_2 treatments at Day 5, but failed to reach statistical significance ($p = 0.093$; Figure 3.5 E). These decreases in *TFB1M* and *TFB2M* did not persist following normoxic recovery ($p > 0.05$; Figure 3.5 D, E).
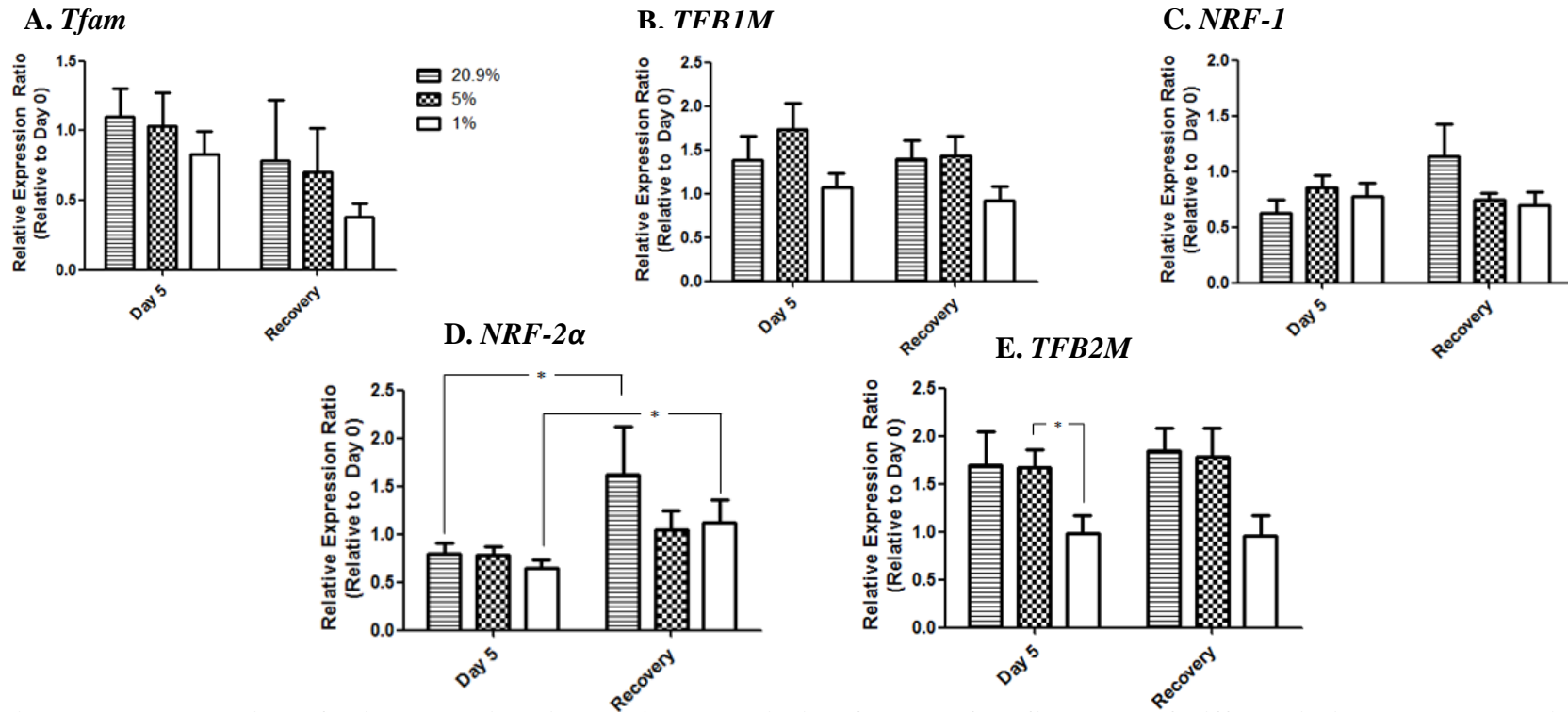
Figure 3.5. Expression of mitochondrial biogenesis transcription factors after five days of differentiation under hypoxia and two days of normoxic recovery. Levels of mRNA for mitochondrial biogenesis genes were analyzed by qRT-PCR and normalized to Day 0. Data were analyzed by a Two-way ANOVA and Tukey's post-hoc test. No significant change was observed for *Tfam* (A), *TFB1M* (B) or *NRF-1* (C). Connecting lines indicate a significant difference between those values for mRNA levels of *NRF-2α* (D) and *TFB2M* (C; * $p<0.05$; n = 4 – 10/experimental group). All data presented as mean ± SEM.

3.3 Effects of RSV on mitochondrial function in hypoxic skeletal muscle cells

3.3.1 RSV effect on hypoxia-induced reductions in oxygen consumption rates

In order to investigate whether a 50 μM RSV treatment could increase oxygen consumption rates in hypoxic cells during recovery under normoxia, O_2 consumption rates of C_2C_{12} cells were determined as described in section 3.1.1. These myotubes were allowed to respire at their basal metabolic rate at 200 μM, 50 μM and 10 μM oxygen within the airtight oxygraph chamber. As no differences were observed between the 20.9% and 5% O_2 treatments in all parameters tested previously (see section 3.1 and 3.2), only the 5% O_2 treatment, which more closely parallels fetal normoxia, was used for RSV treatments as a comparison to the 1% O_2 hypoxic treatment in these studies.

In cells that differentiated under 1% O_2, RSV treatment during normoxic recovery significantly increased O_2 consumption rates (measured at 200 μM) by 36% compared to Day 5 ($p < 0.05$; Figure 3.6 A). The vehicle (DMSO) did not induce any significant change in O_2 consumption rates within the 1% O_2 treatment ($p > 0.05$; Figure 3.6 A). This positive RSV effect was also observed at 10 μM O_2, where RSV increased O_2 consumption rates within the cells that differentiated under 5% O_2 by 46% when compared with Day 5 ($p < 0.01$; Figure 3.6 C). Again, DMSO did not induce any significant change in O_2 consumption rates within the 5% O_2 treatment ($p > 0.05$).

As observed in section 3.1.1 at 200 μM O_2, hypoxia may have permanently lowered O_2 consumption rates as there was an indication that the 1% treatment had a lower O_2 consumption rate than the 5% treatment at Day 5 ($p = 0.073$) and in the recovery DMSO condition ($p = 0.052$; Figure 3.6 A) but these failed to reach statistical significance.

This decrease was maintained at 50 µM O_2 in the recovery DMSO treatment where the 1% O_2 treatment displayed a significantly lower O_2 consumption rate by 29% than the 5% O_2 treatment ($p<0.05$; Figure 3.6 B) as previously observed in the recovery condition in section 3.1.1. Finally, as previously observed, at 10 µM the 1% treatment O_2 consumption rate was significantly lower by 50% than the 5% treatment after five days of differentiation ($p<0.05$; Figure 3.6 C).

RSV treatment during normoxic recovery did not display increases in O_2 consumption rates at 50 µM as suggested by a significantly lower O_2 consumption rate by 44% of the 1% treatment when compared to the 5% O_2 treatment ($p<0.01$; Figure 3.6 B). This finding was compounded by the fact that there were no significant differences within the 1% O_2 treatment between Day 5, recovery with DMSO or recovery with RSV ($p>0.05$). In addition, RSV was not effective within the 5% O_2 treatment at 50 µM O_2, as the Day 5 O_2 consumption rate was significantly lower than both the recovery DMSO ($p<0.05$), and recovery RSV ($p<0.001$) conditions by 42% and 44%, respectively; however, no difference was found between the DMSO and RSV conditions ($p>0.05$; Figure 3.6 B). Finally, at 10 µM, RSV did not have an effect on the 1% O_2 treatment as the Day 5 O_2 consumption rate was significantly lower than the 1% treatment of both recovery DMSO by 63% ($p<0.01$) and recovery RSV by 69% ($p<0.001$; Figure 3.6 C).

3.3.2 RSV negatively affects cell viability

There were a significantly lower number of viable cells following normoxic DMSO treatment of cells which differentiated under 1% O_2 compared with the 5% O_2 treatment (Figure 3.7 A). Within the 1% O_2 treatment, DMSO also significantly

decreased the number of viable cells between Day 5 and recovery ($p < 0.05$ Figure 3.7 A). Beyond the effect of the vehicle, RSV further decreased the number of viable cells within the 5% treatment when compared with Day 5 ($p < 0.01$) and normoxic recovery with DMSO ($p < 0.05$), and within the 1% treatment when compared to Day 5 ($p < 0.01$; Figure 3.7 A). Hypoxia alone had no effect on cell viability after five days of differentiation ($p > 0.05$; Figure 3.7 A).

3.3.3 RSV increases mitochondrial abundance

The decline of CS activity observed following five days of differentiation under 1% O_2 was alleviated following normoxic recovery with RSV treatment showing a 73% increase in the hypoxic condition ($p < 0.01$; Figure 3.7 B). Within the 5% O_2 treatment, this pattern was also apparent, but high variability prevented RSV treatment reaching statistical significance ($p = 0.088$; Figure 3.7 B). This increase in mitochondrial abundance was confirmed by mitotracker where mean fluorescence after a two day recovery period with RSV increased within the 1% treatment by 36% ($p < 0.05$) and within the 5% treatment by 50% ($p < 0.05$) when both were compared with Day 5 (Figure 3.7 B).

3.4 Effects of RSV on hypoxic skeletal muscle cell mRNA and protein

3.4.1 RSV does not affect mitochondrial complex I NDUFB8 protein levels

NDUFB8 protein levels were analyzed as described in section 3.2.1. Differentiation for five days under hypoxia significantly reduced NDUFB8 levels by 50% when compared to the 5% O_2 treatment ($p < 0.05$; Figure 3.8). RSV had no effect on

NDUFB8 levels in the 1% and 5% O_2 treatments (p>0.05; Figure 3.8). Furthermore, no changes in the other subunits of the ETC complexes II − V were observed (data not shown).

3.4.2 RSV increases expression of some mitochondrial biogenesis transcription factors and co-activators

No significant differences were found for *Tfam*, *TFB1M* or *TFB2M* between any O_2 treatment at Day 5 or recovery (p>0.05; Figure 3.9 A, B, C). RSV significantly increased *NRF-1* mRNA levels of the 5% O_2 treatment when compared to both Day 5 (p<0.05) and recovery DMSO (p<0.05) by 51% and 47%, respectively (Figure 3.9 D). RSV also increased *NRF-2α* mRNA levels of the 5% O_2 treatment when compared to both Day 5 (p<0.01) and recovery DMSO (p<0.05) by 42% and 34%, respectively (Figure 3.9 E). In contrast, RSV did not increase *NRF-2α* mRNA levels of the hypoxic cells as there was a significant 27% decrease within the recovery RSV condition observed when compared to the 5% O_2 treatment (p<0.05; Figure 3.5 E).

The mRNA levels of selected mitochondrial biogenesis co-activators were also evaluated before and after RSV treatment. *PGC-1α* mRNA levels were unaffected by hypoxia and RSV treatment (p>0.05 Figure 3.10 A). However, after RSV treatment during normoxic recovery, both the 5% O_2 and 1% O_2 cells displayed significantly increased *PGC-1β* levels by 54% and 44%, respectively, when compared to their Day 5 levels (p<0.05 Figure 3.10 B). This suggests that *PGC-1β* expression was increased by RSV treatment.
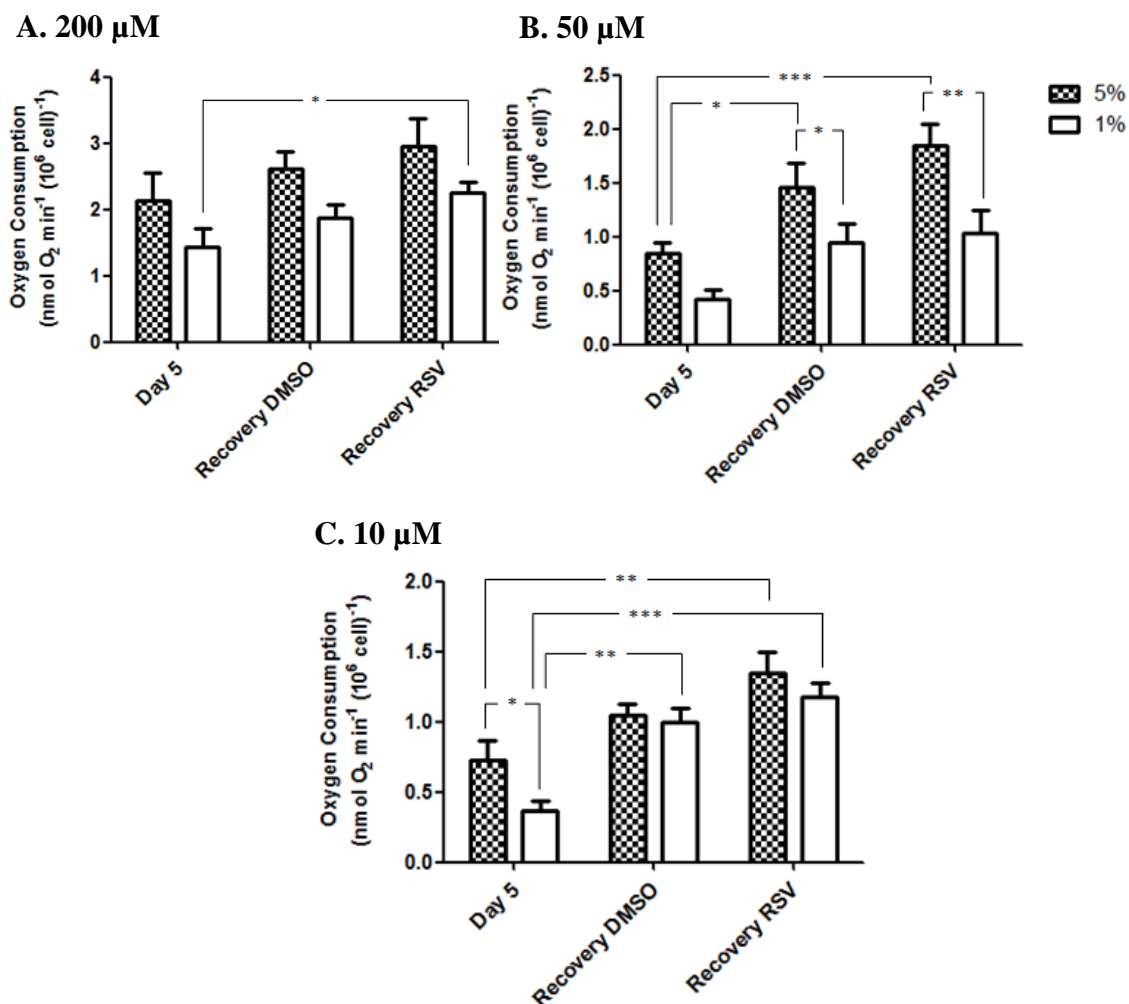
Figure 3.6. Oxygen consumption rates of skeletal muscle cells at varying oxygen concentrations following differentiation under hypoxia and recovery at normoxia with either DMSO or RSV treatment. Oxygen consumption rates were measured by closed-cell respirometry using an Oxygraph-2k Clark-type electrode at 37°C in a 10 mM glucose solution. Data displayed for chamber O_2 concentrations of (A) 200 µM (approximately 20.9% O_2), (B) 50 µM (approximately 5% O_2) and (C) 10 µM (approximately 1% O_2). All data presented as mean ± SEM. Connecting lines indicate a significant difference between those values as determined by a two-way ANOVA with a Tukey's post-hoc test (* $p<0.05$; ** $p<0.01$; *** $p<0.001$; n = 4 – 9/experimental group).
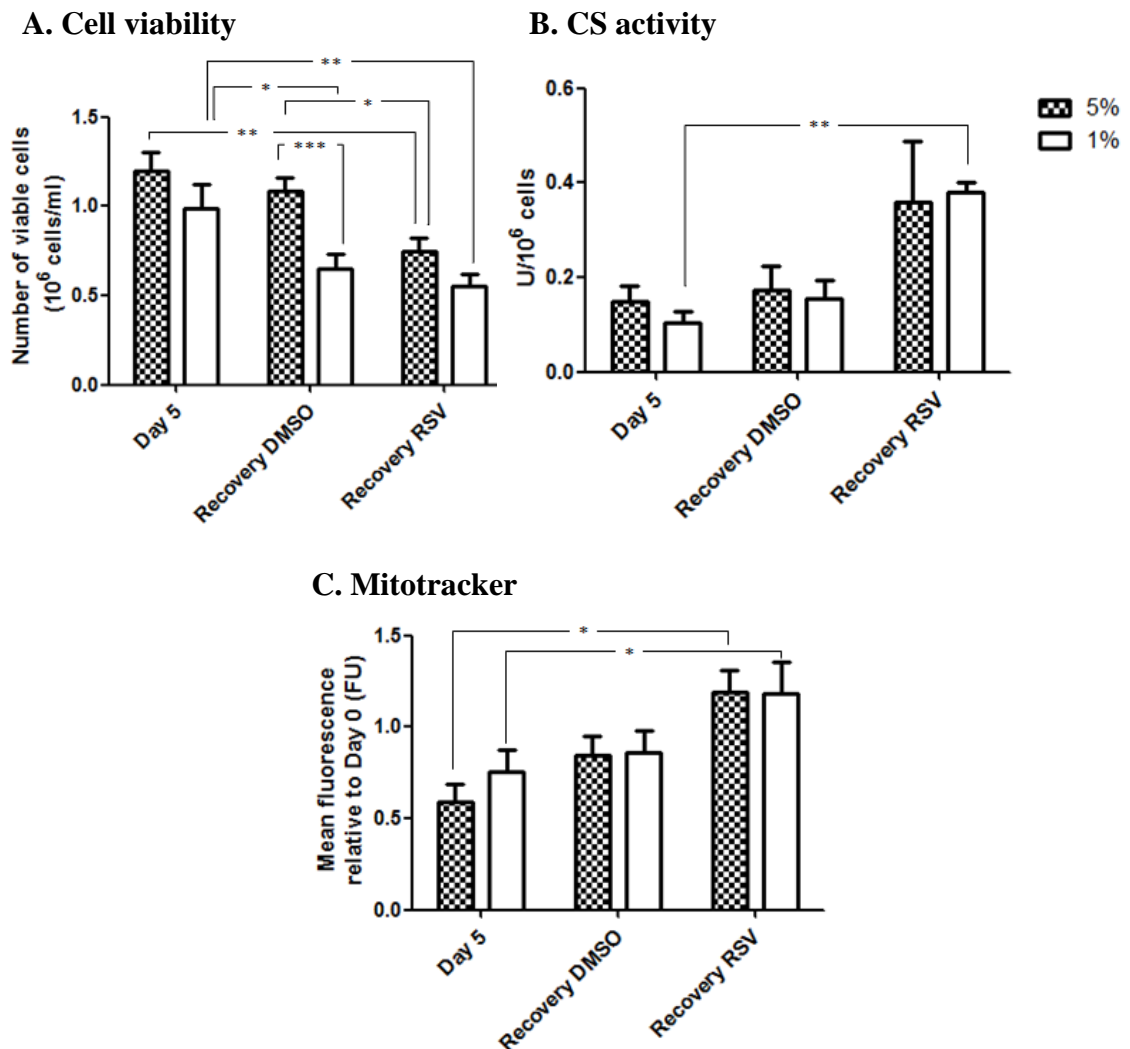
Figure 3.7. Cell viability and mitochondrial abundance are affected by RSV treatment. Cell viability was analyzed using a haemocytometer and a trypan blue stain (A; n = 6 - 9/experimental group). Mitochondrial number and activity was analyzed using a CS activity assay (B; n = 3 − 6/experimental group). Mitochondrial number was further analyzed using flow cytometry and the fluorescent probe Mitotracker and set relative to Day 0 (C; n = 6 − 11/experimental group). All data presented as mean ± SEM. Connecting lines indicate a significant difference between those values as determined by a two-way ANOVA with a Tukey's post-hoc test (* $p<0.05$; ** $p<0.01$; *** $p<0.001$).
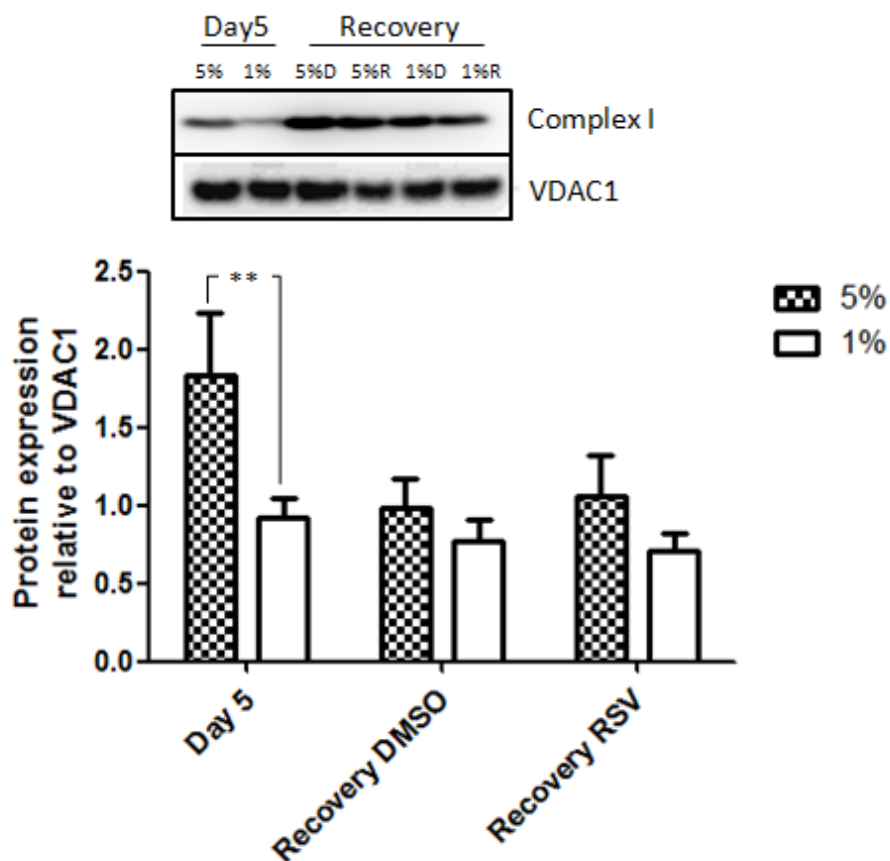
Figure 3.8. Protein levels of NDUFB8, a subunit of complex I, are not affected by RSV treatment. Complex I protein levels were analyzed by Western blot analysis with the antibody for NDUFB8, a nuclear encoded subunit of Complex I. These levels were normalized to VDAC1, an outer mitochondrial membrane protein normalizing for the amount of mitochondrial protein, and analyzed with a Two-way ANOVA with a Tukey's post-hoc test. A representative blot for NDUFB8 and VDAC1 are displayed above the graph. There was a significant depression of the 1% treatment protein levels when compared to the 5% oxygen treatment at Day 5 (** $p < 0.01$; n = 6 − 9/experimental group). All data presented as mean ± SEM.

49
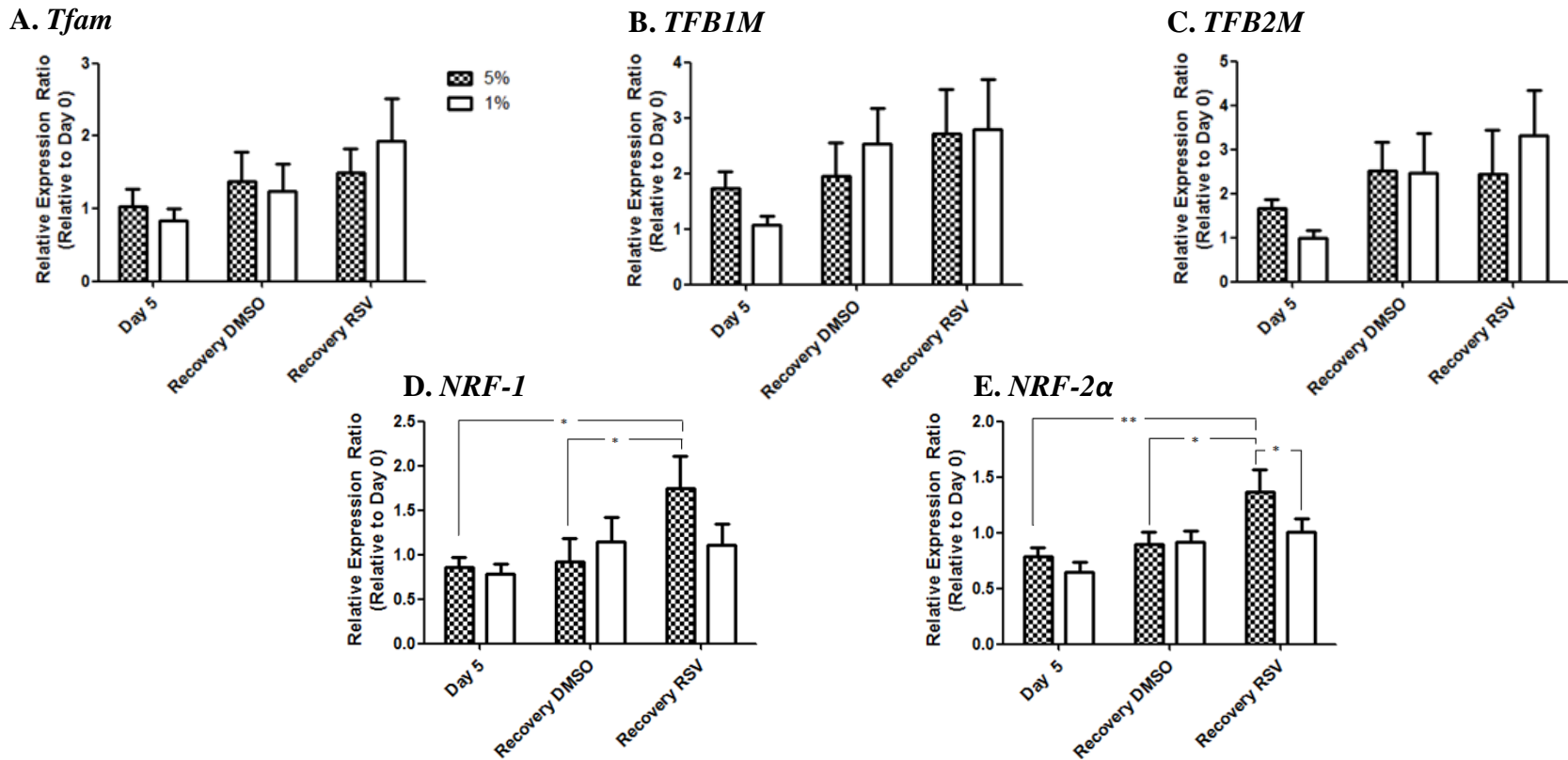
Figure 3.9. RSV increases mRNA levels of mitochondrial biogenesis transcription factors, but not in hypoxic skeletal muscle cells. Levels of mRNA for mitochondrial biogenesis genes were analyzed by qRT-PCR and normalized to Day 0. Data were analyzed by a Two-way ANOVA and Tukey's post-hoc test. No significant change was observed for *Tfam* (A), *TFB1M* (B) or *TFB2M* (C). Connecting lines indicate a significant difference between those values for mRNA levels of *NRF-1* (D) and *NRF-2α* (C; * p<0.05; **p<0.01; n = 5 – 11/experimental group). All data presented as mean ± SEM.

A. *PGC-1α*
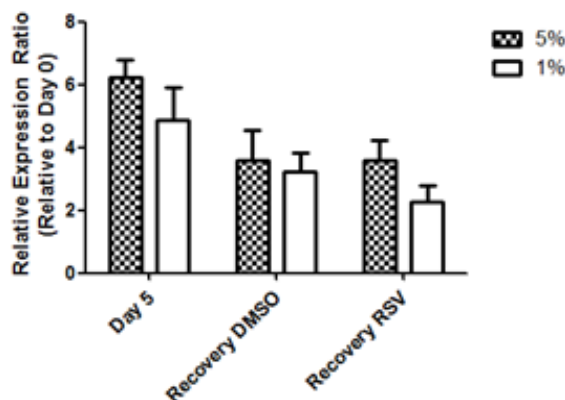
B. *PGC-1β*
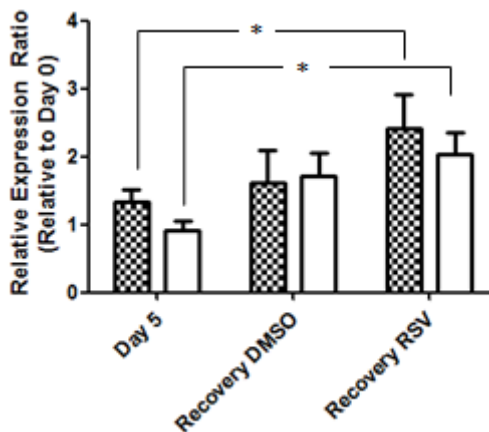
Figure 3.10. The mRNA levels of co-activators of mitochondrial biogenesis are unaffected by hypoxia, but increase with treatment of RSV during a two day normoxic recovery. Levels of mRNA for mitochondrial co-activators were analyzed by qRT-PCR and normalized to Day 0. Data was analyzed by a Two-way ANOVA and Tukey's post-hoc test. No significant change was observed for *PGC-1α* after five days of hypoxia or with RSV treatment during recovery (A). Connecting lines indicate a significant difference between those values for mRNA levels of *PGC-1β* with RSV treatment (B; * $p<0.05$; n = 6 − 11/experimental group). All data presented as mean ± SEM.

Chapter 4: Discussion

Current research suggests that babies born IUGR are more susceptible to metabolic diseases such as insulin resistance in adulthood (Jaquet *et al*., 2000; Hales *et al.*, 1991). IUGR offspring develop as a result of placental insufficiency, characterized by low placental glucose and O_2 transfer from maternal to fetal circulation which results in reduced delivery to the fetus, and is a major contributor to the development of IUGR (Baschat, 2004; Pardi *et al*., 2002). Oxygenation alone has profound effects on fetal development (Giussani *et al*., 2007), such as preferentially redistributing blood flow to major organs such as the heart, brain and adrenals (Arbeille et al., 1995) presumably increasing fetal survival. In IUGR fetuses, however, this blood redistribution is thought to result in morphological and metabolic alterations to peripheral tissues, such as skeletal muscle, which could cause long-term impairments postnatally.

Skeletal muscle dysfunction alters glucose metabolism, which is associated with the development of insulin resistance and type 2 diabetes (Selak *et al*., 2003, Patti *et al*., 2003). Skeletal muscle exposed to hypoxia *in utero* or in cell culture display decreases in skeletal muscle cell respiration (Selak *et al*., 2003; Arthur *et al*., 2000; Lane *et al*., 1998), a reduction in factors involved in mitochondrial biogenesis (Regnault *et al*., 2010) and mitochondrial proteins (Lane *et al*., 1998), suggesting mitochondrial dysfunction is altered during a hypoxic insult. Therefore, I investigated alterations in skeletal muscle metabolism. Specifically, I sought to examine whether hypoxia during differentiation of skeletal muscle cells affected oxidative metabolism and mitochondrial biogenesis, and whether any alterations persist after recovery from hypoxia. Furthermore, I studied if

RSV, a pharmacological intervention which increases mitochondrial biogenesis (Park *et al*., 2012), is able to promote recovery from the hypoxic insult.

4.1 Role of hypoxia in altering skeletal muscle OXPHOS

Oxygen consumption rates of mouse C_2C_{12} skeletal muscle cells were depressed following five days of differentiation under 1% O_2 when compared to both the 5% and 20.9% controls (Figure 3.1 A – C). This hypoxic suppression of O_2 consumption of hypoxic cells persisted even after the hypoxic insult was alleviated by two days of normoxic recovery. Interestingly, this change in O_2 consumption rate was not associated with decreases in cell viability or mitochondrial abundance as these were not affected in the hypoxic treatment. In reports of mouse 32D myeloid cells cultured under normoxic conditions, the "apparent Km" of respiration for O_2 was determined to be 0.5 μM (Scandurra and Gnaiger, 2010), 20-fold lower than the 1% O_2 concentration of my hypoxic treatment. Therefore, it might be assumed that the decreased O_2 consumption rate displayed by my cells incubated at 1% O_2 was not the result of O_2 limitation of complex IV, but rather a controlled down-regulation of mitochondrial metabolism in response to chronic (five days) hypoxia. Furthermore, my results suggest that hypoxia-induced alterations to O_2 consumption have permanent consequences. Previous studies have demonstrated that C_2C_{12} cells display rapid decreases in O_2 consumption with decreases in O_2 concentration, although, these cells returned to normoxic O_2 consumption rates upon re-oxygenation (Arthur *et al*., 2000). This study however, investigated acute changes (no longer than three hours) in skeletal muscle O_2 consumption while my study

demonstrated that a chronic five day hypoxic insult results in a sustained suppression of O_2 consumption for at least 48 hours of re-oxygenation.

Reducing O_2 consumption during hypoxia is advantageous as it would aid in increasing survival of skeletal muscle cells by reducing hypoxia-induced signaling cascades which lead to DNA damage and apoptosis (Greijer and van der Wall, 2003). A major consequence of hypoxic signaling is a reduction of OXPHOS, a major consumer of O_2 within the cell (Papandreou *et al.*, 2006). Skeletal muscle isolated postnatally from IUGR rat offspring displayed reductions in OXPHOS capacity (Selak *et al.*, 2003). In this case, a model of placental insufficiency by reducing blood flow through the uterine artery was used; therefore, these IUGR rat fetuses were displaying the compounding effects of decreased O_2 and nutrient supply. My study determined that hypoxia alone is sufficient to cause these potentially permanent reductions in skeletal muscle O_2 consumption.

The ETC, a major consumer of O_2 within the cell by OXPHOS, was examined in this study to determine if the reduced O_2 consumption observed during and after hypoxia was associated with alterations in the complexes as there was no hypoxic effect on mitochondrial abundance or cell viability (Figure 3.2 A - C). Complex I is a multi-subunit protein and is derived from both mitochondrial and nuclear genes (Scarpulla, 2008; Caroll *et al.*, 2003). In this study, an established antibody directed against NDUFB8, a nuclear encoded subunit of complex I, was used to determine protein levels of complex I. This antibody was part of a cocktail of five antibodies which was used to evaluate the protein levels of all the complexes of the ETC. Of this cocktail only NDUFB8 protein levels were reduced after five days of differentiation under hypoxia (Figure 3.4) while no other complexes of the ETC were altered by hypoxia which suggests that complex I alone was a target of hypoxia-induced alterations. Decreases in complex I activity would decrease

O_2 consumption rates as there would be a reduction in the rate of electrons entering the ETC. This decrease would not only help maintain the already low O_2 levels, but also may attenuate the initial burst of ROS being produced by the ETC that presumably occurred at the onset of hypoxia.

ROS have a major role in hypoxic signaling (Hoppeler *et al.,* 2003; Chandel *et al*., 2000), and the mitochondria is suggested to be the source of ROS under hypoxia (Guzy *et al*., 2005; Anderson and Neufer, 2005; Schroedl *et al.,* 2002; Chandel *et al.,* 1998; Vanden Hoek *et al.,* 1998). Despite this, I found that differentiation under hypoxia did not increase ROS at the level of either the whole cell or mitochondria when compared to 20.9% and 5% O_2 controls (Figure 3.3 A, B). However, high levels of ROS within the cell can also be damaging, which is most likely why hypoxic bursts in ROS levels are acute and begin to decline within an hour of the onset of hypoxia (Chandel *et al.,* 1998). My experimental design sampled skeletal muscle cells after five days of differentiation under hypoxia and would not have detected these early bursts of ROS, which may be due to decreases in NDUFB8 protein and the O_2 consumption rate. Presumably, C_2C_{12} cells would display an increase in ROS levels within an hour of exposure to hypoxia (Chandel *et al*. 1998) as has been observed in previous studies of isolated rat skeletal muscle (Zuo and Clanton, 2005), which is linked to hypoxic signaling by HIF-1α (Chandel *et al*., 2000).

Following two days of normoxic recovery, NDUFB8 protein levels in the hypoxic (1% O_2) treatment remained low, but were no longer significantly lower than the 5% and 20.9% O_2 treatments (Figure 3.4). This result likely reflects slight decreases in the 5% and 20.9% NDUFB8 protein levels compared with the Day 5 levels, which was not found in the 1% O_2 treatment. My data show a decrease in NDUFB8 under chronic hypoxia, which

was not reversed upon re-oxygenation. Interestingly, previous studies reported that hypoxia decreased expression of complex I subunits derived from mtDNA and complex I activity (Piurat and Lopez-Barneo, 2005). This hypoxic suppression of complex I was reversible upon re-oxygenation (Piurat and Lopez-Barneo, 2005). This study, however, exposed cells to hypoxia for no longer than 24 hours while my study investigated the effects of a chronic five day hypoxic incubation on NDUFB8 protein levels. Previous studies have suggested that alterations in ETC complex I subunits are plastic (Piurat and Lopez-Barneo, 2005). This plasticity could result from post-translational mechanisms induced by HIF-1α which selectively target complex I. Increased stabilization of HIF-1α during hypoxia increased expression of NDUFA4L2 and microRNA-210 which reduced complex I activity and protein levels, respectively (Tello *et al.*, 2011; Chan *et al.*, 2009). NDUFA4L2 and microRNA-210 could be two hypoxia-specific mechanisms active in my model by which complex I subunits are altered, and their expression would be attenuated upon re-oxygenation and degradation of HIF-1α allowing for NDUFB8 to recover. Although NDUFA4L2 and microRNA-210 may be active in my system during the hypoxic insult, further research is necessary to determine if these are contributing factors to maintaining low levels of NDUFB8 after normoxic recovery.

Upstream factors of OXPHOS may have been altered during hypoxia and could contribute to the persistent suppression of the O_2 consumption rates of hypoxic cells following normoxic recovery. Decreased PDH activity would restrict substrate supply to the ETC, potentially decreasing O_2 consumption rates. HIF-1α suppressed PDH levels by increasing PDHK levels (Papandreou et al., 2006). In addition, in rat models of IUGR, decreases in PDH activity and increases in PDHK of skeletal muscle were maintained into early adulthood when compared to controls (Selak *et al.*, 2003). In my study, glucose

was used as the sole oxidative substrate for measurements of O_2 consumption rates and the activity of PDH could therefore exert considerable control over O_2 consumption rates. Hypoxia alone initiated increases in PDHK (Papandreou *et al.*, 2006), and this could be a mechanism that suppressed O_2 consumption rates in hypoxic skeletal muscle cells even after exposure to two days of normoxia. Examinations of hypoxic C_2C_{12} skeletal muscle levels of PDH and PDHK would determine if alterations in PDH contribute to the altered O_2 consumption rates.

Decreases in mitochondrial biogenesis could also contribute to alterations in skeletal muscle O_2 consumption. Alterations in factors associated with mitochondrial biogenesis have been observed in skeletal muscle of *in vitro* models (Regnault *et al*., 2010) and in adults with insulin resistance (Patti *et al*., 2003). In my study mRNA levels of the nuclear transcription factors involved in mitochondrial biogenesis, *NRF-1* and *NRF-2α*, were unaffected by hypoxia (Figure 3.5 D, C). There was a rise in mRNA levels of *NRF-2α* in both the 20.9% O_2 control and 1% O_2 hypoxic treatments post-recovery, which can be attributed to continued differentiation and associated increases in mitochondrial biogenesis (Duguez *et al*. 2001). Although there were no changes in the nuclear transcription factors studied, other nuclear transcription factors could be affected by hypoxia such as the estrogen-related receptor α (ERR-α; Schreiber *et al*., 2004). ERR-α is involved in the expression of nuclear oxidative phosphorylation genes and mitochondrial biogenesis with separate DNA binding sites than NRF-1 and NRF-2α (Schreiber *et al*., 2004; Mootha *et al*., 2004). There was, however, a significant reduction in the mRNA levels of *TFB2M* following five days of differentiation under hypoxia when compared to controls (Figure 3.5 E). *TFB2M* is involved in both mtDNA transcription and replication (Cotney *et al*. 2007; Scarpulla, 2006); therefore it can be assumed that

reductions in *TFB2M* would contribute to decreases in mitochondrial biogenesis. In my study I did not observe alterations in mitochondrial abundance as indicated by mitotracker and citrate synthase enzyme activity after five days of differentiation under hypoxia when compared to controls. This could potentially be attributed to slow turnover of mitochondria, ranging from 4 to 24 days, that was reported in other cell types (Lipsky and Pedersen, 1981; Menzies and Gold, 1971). If these C_2C_{12} cells were allowed to grow beyond the seven days of differentiation in this study, decreases in mitochondrial abundance may be observed.

Any alterations in the mRNA of mitochondrial biogenesis factors that were analyzed in my study did not persist following recovery in normoxic conditions. Previous whole animal studies have implicated alterations in mitochondrial biogenesis factors in IUGR pig offspring postnatally, including decreases in mRNA levels of *Tfam* and *NRF-1*; however, these alterations were only pronounced when a high fat diet was fed to these IUGR pigs postnatally (Liu *et al*., 2012). Potentially hypoxia alone is not sufficient to decrease mRNA levels of these mitochondrial biogenesis factors and is also dependent on nutritional factors.

4.2 RSV is not an effective pharmacological intervention for reversing hypoxic-induced alterations in cultured skeletal muscle cells.

RSV is a known antioxidant (Mahal and Mukherjee, 2006) and has protective effects on skeletal muscle during ischemia and reperfusion (Ikizler *et al*., 2006). Furthermore RSV activates an AMPK pathway which increases PGC-1α protein and activity (Park *et al*., 2012); PGC-1α co-activates mitochondrial biogenesis factors such as

NRF-1 and NRF-2α (Scarpulla, 2006). RSV appears to be an ideal pharmacological intervention for mitochondrial dysfunction diseases as it can promote increases in the mitochondrial biogenesis pathway and mitochondrial abundance, ultimately improving oxidative metabolism. Indeed, in mice treated with RSV, isolated heart mitochondria (Gutierrez-Perez *et al*., 2011) and muscle fibers (Lagouge *et al*., 2006) displayed an increased aerobic capacity. Oxygen consumption in my hypoxic (1% O_2) and 5% O_2 skeletal muscle cells increased with RSV treatment during normoxic recovery. However, this increase was only observed at 200 μM O_2 for the 1% O_2 (Figure 3.6 A) treatment and 10 μM for the 5% O_2 treatment (Figure 3.6 C). This suggests that RSV does have a positive effect on increasing O_2 consumption rates of hypoxic cells, but the effect is not consistent. Previous research investigating the effects of RSV on C_2C_{12} skeletal muscle cells observed increases in the O_2 consumption rate with treatment of 50μM RSV (Park *et al*., 2012). The C_2C_{12} cells in Park *et al*. (2012), however, were not pre-treated with hypoxia which is unlike my study. This may indicate that RSV treatment on C_2C_{12} cells which differentiated under lower O_2 concentrations does not activate the AMPK pathway the same as cells which differentiate under 20.9% O_2 (Park *et al*., 2012). RSV treatment after a hypoxic-insult in skeletal muscle cell O_2 consumption rates has not been extensively researched and requires further study as it may have different effects than previously found in normoxic conditions.

In this study, RSV was applied to the 5% and 1% O_2 treatments for the full 48 hours of re-oxygenation following five days of differentiation under 5% or 1% O_2. As discussed previously, oxidative bursts in ROS may have an important role in re-oxygenation states as well as hypoxic states. In primary cultured hepatocytes, increases in ROS during re-oxygenation aided factors important for increasing cell survival, and

antioxidants inhibited this effect and were associated with increases in apoptosis during this re-oxygenation (Terui *et al*., 2004). As both the 1% and 5% O_2 treatment would experience a re-oxygenation process in the recovery condition, bursts in ROS could potentially occur. It is possible that the antioxidant properties of RSV prevented anti-apoptotic ROS-signaling during re-oxygenation. The lack of consistent increases in the aerobic capacity of the 1% and 5% O_2 may have been impacted by alterations in cell viability brought on by a decrease in cell survival during re-oxygenation.

Despite the alterations in the number of viable cells (Figure 3.7 A), RSV induced an increase in mitochondrial abundance as indicated by increases in citrate synthase activity and mitotracker accumulation in both the 5% and 1% O_2 treatments (Figure 3.7 B, C). This coincides with previous RSV research which observed increases in mtDNA, related to increases in mitochondrial abundance in both *in vitro* (Park *et al*., 2012) and *in vivo* (Lagouge *et al*., 2006) systems. This suggests that mitochondrial biogenesis in the hypoxic and 5% O_2 treated C_2C_{12} cells was induced with RSV treatment during recovery. My molecular data confirms these results, as RSV treatment during recovery of cells that differentiated under 5% O_2 displayed increased mRNA levels of the nuclear transcription factors *NRF-1* and *NRF-2α* (Figure 3.9 D, E). This coincides with previous research which reported increases in *NRF-1* in cultured endothelial cells (Csiszar *et al*., 2009), isolated mice aortas (Csiszar *et al*., 2009) and mouse skeletal muscle (Lagouge *et al*., 2006) with RSV treatment which promoted mitochondrial biogenesis. However, at 1% O_2, RSV did not alter expression of these genes and *NRF-2α* was actually significantly lower than the 5% O_2 treatment. This significant decrease in *NRF-2α* is most likely due to the increase observed in the 5% treatment with RSV, augmenting the difference, and not a depression of the 1% O_2 treatment mRNA levels due to RSV. This result suggests

expression of some mitochondrial biogenesis factors may be permanently affected by differentiation under more severe hypoxia. Increases in mitochondrial abundance in the hypoxic cells may instead be attributed to other mitochondrial biogenesis factors such as PGC-1β, a mitochondrial biogenesis co-activator. PGC-1β, like PGC-1α, is a potent co-activator of NRF-1 active in skeletal muscle which leads to increased expression of mitochondrial gene (Scarpulla, 2006) and would be expected to increase with RSV treatment. Indeed, *PGC-1β* mRNA levels were increased in both the 5% and 1% O_2 treatments (Figure 3.10 B). Increased *PGC-1β* expression and transcriptional complex binding to NRF-1 would be associated with the increases in mitochondrial abundance that was observed in the hypoxic cells. The resultant increases in mitochondrial abundance could account for the recovery of the oxygen consumption rates of skeletal muscle cells exposed to a chronic hypoxic insult. Further research, however, is necessary to investigate the differential expression of mitochondrial biogenesis markers with RSV treatment on cells pre-treated with hypoxia.

Paradoxically, while RSV mediated increases in mitochondrial abundance in both O_2 treatments, it did not selectively increase NDUFB8 protein levels (Figure 3.8). This finding does not agree with previous research as increases in complex I subunits were reported in cultured endothelial cells (Csiszar *et al*., 2009) and *in vivo* in isolated mouse muscle cells (Lagouge *et al*., 2006). Neither of these studies, however, employed hypoxia perhaps accounting for the discrepancies with my results. Furthermore, in my study NDUFB8 levels were standardized to levels of mitochondrial protein as determined by VDAC1. It may be that increases in complex I subunit levels are not selectively increased by RSV, and instead only increase with mitochondrial numbers by mitochondrial biogenesis. Previous studies have investigated relative mRNA expression (Lagouge *et al*.,

2006), or complex I levels relative to total cell protein (Csiszar *et al*., 2009), which are not normalized to mitochondrial number or protein. Potentially, in these studies, increases in complex I were detected because of increases in mitochondrial abundance, and were not associated with increases of subunits of complex I protein selectively.

4.3 Conclusions

In agreement with my hypothesis, skeletal muscle differentiation under five days of chronic hypoxia in cell culture caused a decrease in cellular O_2 consumption rates that was maintained after normoxic recovery. Interestingly, mRNA of mitochondrial biogenesis transcription factors and NDUFB8 protein levels were suppressed during the hypoxic insult, but returned towards control values upon re-oxygenation (Figure 4.1). Rat models of IUGR have displayed similar decreases in aerobic capacity and altered gene and protein expression of skeletal muscle mitochondria which was maintained postnatally (Selak *et al*., 2003; Lane *et al*., 1998). My model suggests that hypoxia contributes to the suppression of O_2 consumption rate in skeletal muscle cells and this persistent decrease could contribute to the altered aerobic capacity observed in rat IUGR models postnatally. These hypoxia-induced alterations may be permanent and would pre-dispose these IUGR infants to later-life diseases such as insulin resistance. Indeed, insulin resistant and type 2 diabetic adults have decreases in oxidative capacities as indicated by decreases in citrate synthase and other oxidative enzyme activities (Simoneau and Kelley, 1997) and decreases in factors of mitochondrial biogenesis (Patti *et al*., 2003). My study suggests that hypoxia, isolated from alterations in nutrition, is sufficient to alter O_2 consumption rates, the ETC and mitochondrial biogenesis in IUGR fetuses. Furthermore, rates may be

permanently altered in these infants postnatally as a two day normoxic recovery of skeletal muscle C_2C_{12} cells did not reverse the hypoxia-induced suppression of O_2 consumption rates. However, it appears alterations in O_2 consumption rates after normoxic recovery were not associated with decreases in complex I NDUFB8 protein levels, but could be related to other factors of OXPHOS such as deficits in PDH protein levels.

In contrast to the hypothesis proposed in this study, RSV was not sufficient in reversing hypoxia-induced alterations in O_2 consumption rates at all oxygen concentrations measured, regardless of the increases in mitochondrial abundance that were observed (Figure 4.1). This may be due to antioxidant effects of RSV treatment during re-oxygenation which decreased cell viability, or could be due to altered RSV action within hypoxic cells. Other studies have had success with RSV treatment in young adult mice (Lagouge *et al*., 2006; Baur and Sinclair, 2006), but these studies were not investigating RSV effects on hypoxia-induced alterations. My study indicates the need for examination of the effects of RSV on hypoxic skeletal muscle cells, its effects during re-oxygenation and how this differs from cultured cells which differentiate under normoxia.
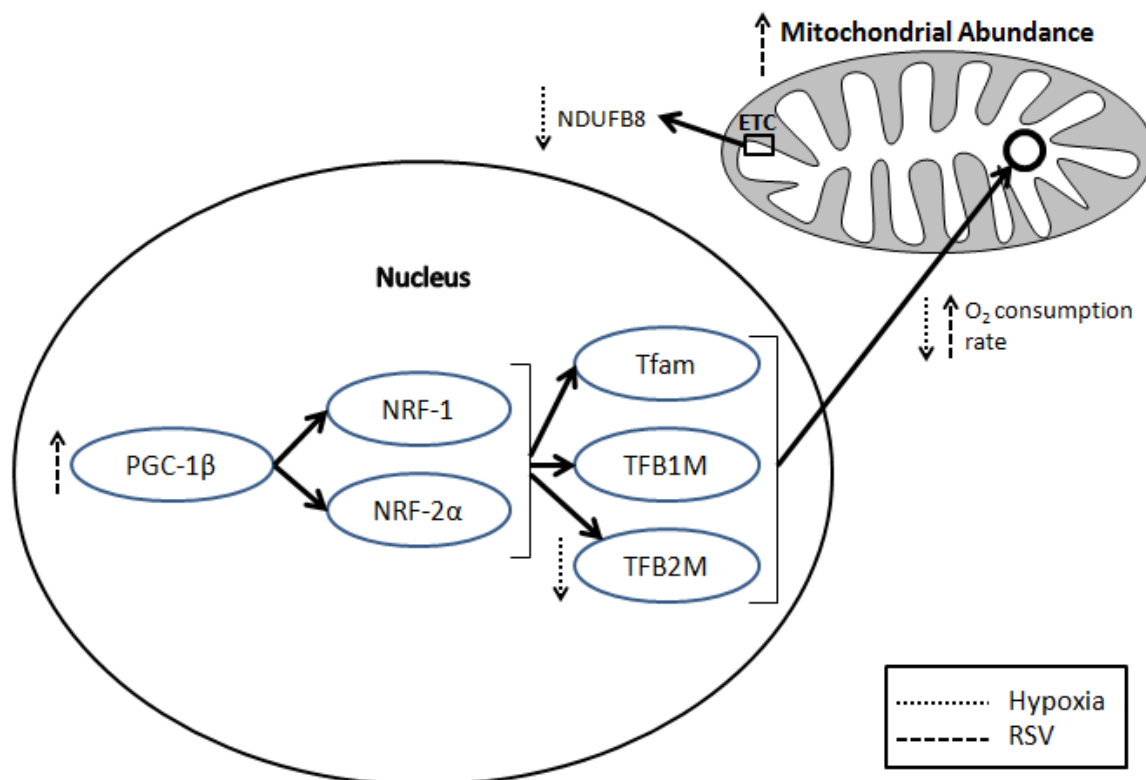
Figure 4.1. Summary of the alterations of skeletal muscle cells which have undergone five days of differentiation incubated at 1% O_2 (hypoxia) and subsequent two days of RSV treatment under normoxia. Arrows indicate an increase or decrease associated with either hypoxic or RSV treatment. Five days of differentiation under hypoxia decreased O_2 consumption rates, protein levels of the NDUFB8 subunit of complex I of the electron transport chain (ETC) and expression of *TFB2M*. The hypoxia-induced decrease in O_2 consumption rates persisted following incubation at normoxia for an additional two days (recovery). Normoxic recovery supplemented with RSV increased oxygen consumption rates, mitochondrial abundance and expression of *PGC-1β*.

4.4 Future studies

This study has highlighted hypoxia during differentiation as a major contributor to alterations in skeletal muscle oxidative metabolism. More importantly, this study suggests that alterations in oxidative metabolism remain after the hypoxic insult is alleviated for 48 hours. Future studies may extend the timeline of the recovery condition to investigate if any recovery occurs, or more importantly, and examine the plasticity of these alterations such as the changes in mitochondrial abundance, that may occur in future time points.

My study implicates O_2 as a major factor in skeletal muscle cell development. Further examination into how hypoxic signaling affects these developing muscle cells may help to elucidate pathways involved in these alterations. Levels of ROS within these cells during the initial hypoxic insult and during re-oxygenation should be investigated as it has implications in both hypoxic signaling and potentially the effects of RSV during re-oxygenation. Other antioxidants, besides RSV, could be applied to this system to elucidate if antioxidants alone can affect cell viability, or if the decrease in the number of viable cells was an RSV-specific effect.

I observed that NDUFB8 levels were suppressed during hypoxia which can have beneficial effects including decreasing ROS levels and conserving O_2 in the cell. Post-translational changes involving NDUFA4L2 or microRNA-210 are factors that can have a role during hypoxic signaling and may have been active in these hypoxic skeletal muscle cells. Hypoxic increases of the levels of microRNA-210 and NDUFA4L2 protein in skeletal muscle cells would indicate that these are active in my model. Because this decrease in complex I levels was not maintained after normoxic recovery when compared to controls, other factors must also contribute to the decrease in the O_2 consumption rates

of these skeletal muscle cells. Some factors that have been implicated in hypoxic signaling are of interest, such as PDH and PDHK, which are known to be affected after HIF-1α stabilization under hypoxia which may be maintained post-hypoxic insult. Protein levels of PDH and PDHK would elucidate whether lowered PDH levels contribute to the decrease in O_2 consumption during hypoxia and normoxic recovery.

Finally, my study into the pharmacological intervention RSV, did have positive effects such as increases in mitochondrial abundance, but my results were not consistent in terms of O_2 consumption rates. Further investigation into the differential effects of RSV between the 20.9% O_2 treatment and the 5% and 1% O_2 treatments may elucidate differences in RSV action in these O_2 treatments. Examination of RSV treated 20.9% O_2 cells of NDUFB8 levels and mRNA levels mitochondrial biogenesis transcription factors analyzed in this study would help to clarify differences among all O_2 treatments. Additionally, attempting to treat these cells with RSV at a later time point than used in this study may help to demonstrate if re-oxygenation plays a role in RSV-mediated effects. RSV treatment for 6 hours has successfully increased O_2 consumption in normoxic C_2C_{12} cells (Park *et al*., 2012), so a shorter RSV treatment could be used in this system and may display more consistent results.

Appendix: Supplemental figures

A.1 Oxygen consumption rates with and without RSV treatment

Oxygen consumption rates were measured as described in section 3.1.1. Oxygen consumption rates of cells which differentiated under 20.9%, 5% and 1% O_2 for five days and during a two day normoxic recovery period were examined at a range of O_2 concentrations (200 µM – 0 µM) within the Oxygraph-2k chamber (Figure A.1). Data were analyzed at 200 µM, 50 µM and 10 µM of O_2.

To confirm RSV activation of O_2 consumption as reported in (Park *et al*., 2012), RSV treatment (50 µM) was applied to the 20.9% O_2 condition for a two day period. Data were analyzed with a one-tailed Student's t-test and a significant increase in the O_2 consumption rate with RSV treatment was observed at 200 µM O_2 ($p<0.05$; Figure A.2 A), but not at lower O_2 concentrations within the chamber ($p>0.05$; Figure A.2 B, C).

A.2 Flow cytometry using BD CFlow software

Example output figures of BD CFlow software which highlights the collection of data during flow cytometry. For each sample, 50,000 events (cells) were recorded and plotted in a frequency distribution which plots forward scatter (FSC-A) on the x-axis and side scatter (SSC-A) on the y-axis (Figure A.3 A, A.4 A). This graph is based on the scattering of light by the cell as it passes by the light source in the flow cytometer. Forward scatter correlates with cell size while side scatter correlates with the complexity of the particle such as shape and granularity; a higher forward scatter value indicates a larger cell, and a higher side scatter value indicates a more complex cell. Controls for

each sample without fluorescent probes were run through the flow cytometer to determine background fluorescence. To organize the data, control samples were used to gate the data to exclude dead cells (low forward and side scatter values) from all further analysis (Figure A.3 B); gates are also applied to their corresponding treated sample (Figure A.4 B). Lastly, a histogram of these gated samples was produced which plotted the fluorescent intensity of each event recorded against the number of times this fluorescent intensity was detected (Figure A.3 C, A.4 C).
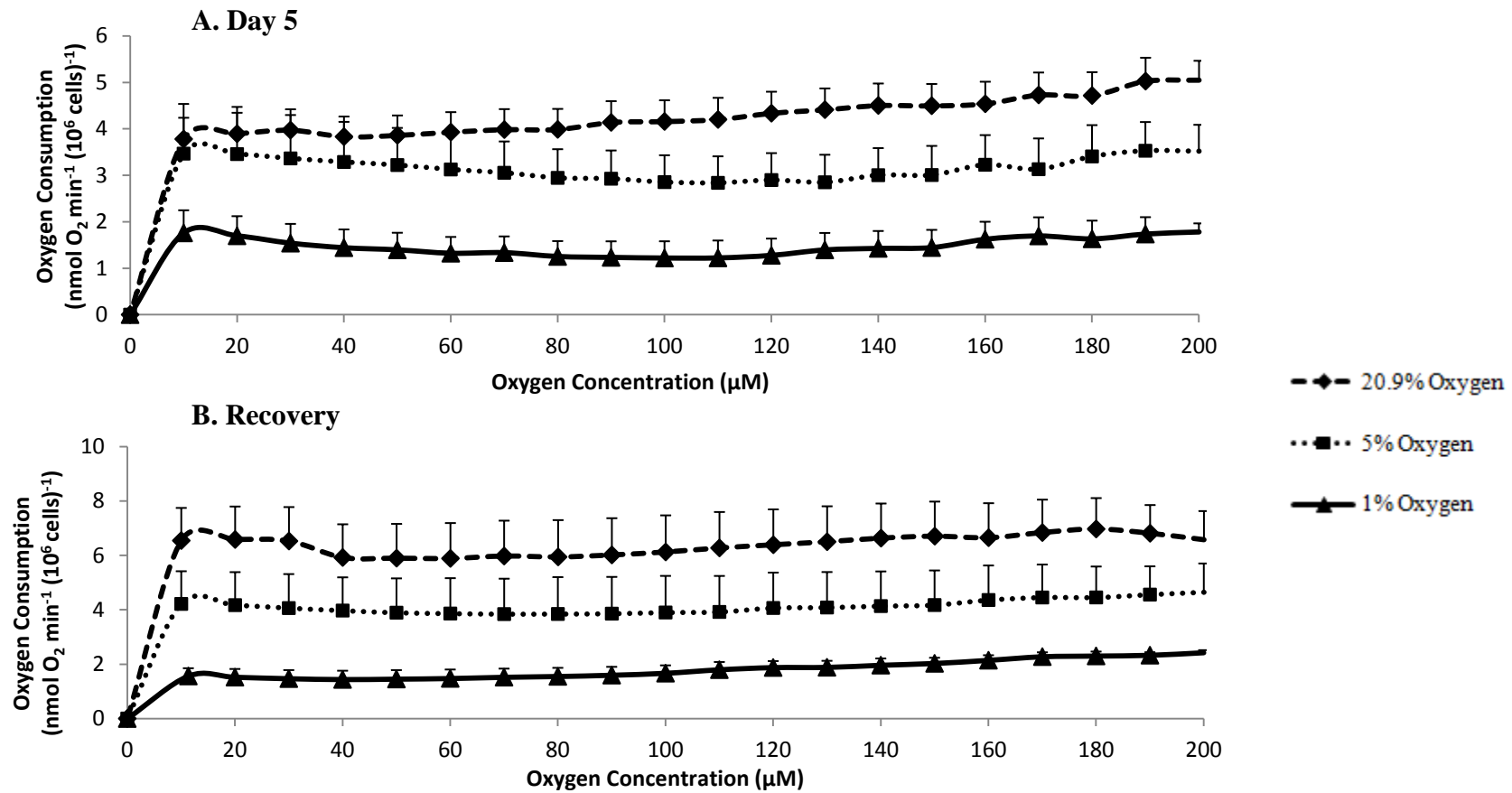
Figure A.1. Oxygen consumption rates of C_2C_{12} skeletal muscle cells over varying O_2 concentrations in the Oxygraph-2k chamber. Oxygen consumption rates after five days of differentiation under 1%, 5% or 20.9% oxygen (A) and after a two day recovery period at 20.9% oxygen (B) are displayed. All data presented as mean ± SEM (n = 6 − 7/experimental group).

A. 200 μM Oxygen

B. 50 μM Oxygen

C. 10 μM Oxygen
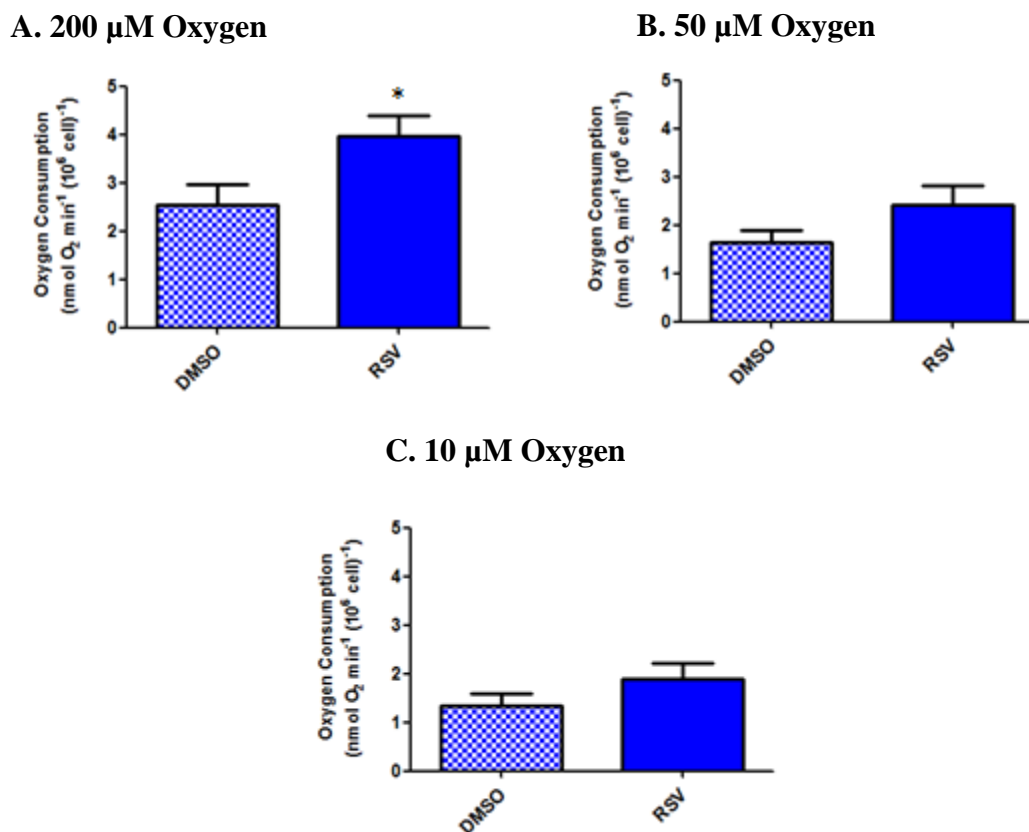
Figure A.2. A two day treatment of RSV increases O_2 consumption rates in cells which differentiated under 20.9% O_2. A 50 μM RSV treatment was applied for two days at 20.9% O_2 to skeletal muscle cells after differentiation under 20.9% O_2 for five days. Oxygen consumption rates were measured by closed-cell respirometry using an Oxygraph-2k Clark-type electrode at 37℃ in a 10 mM glucose solution. Data displayed for chamber O_2 concentrations of (A) 200 μM (approximately 20.9% O_2), (B) 50 μM (approximately 5% O_2) and (C) 10 μM (approximately 1% O_2). All data presented as mean ± SEM. Asterisk indicates a significant difference between those values (* $p<0.05$; n = 4/experimental group).

A.

B.

C.
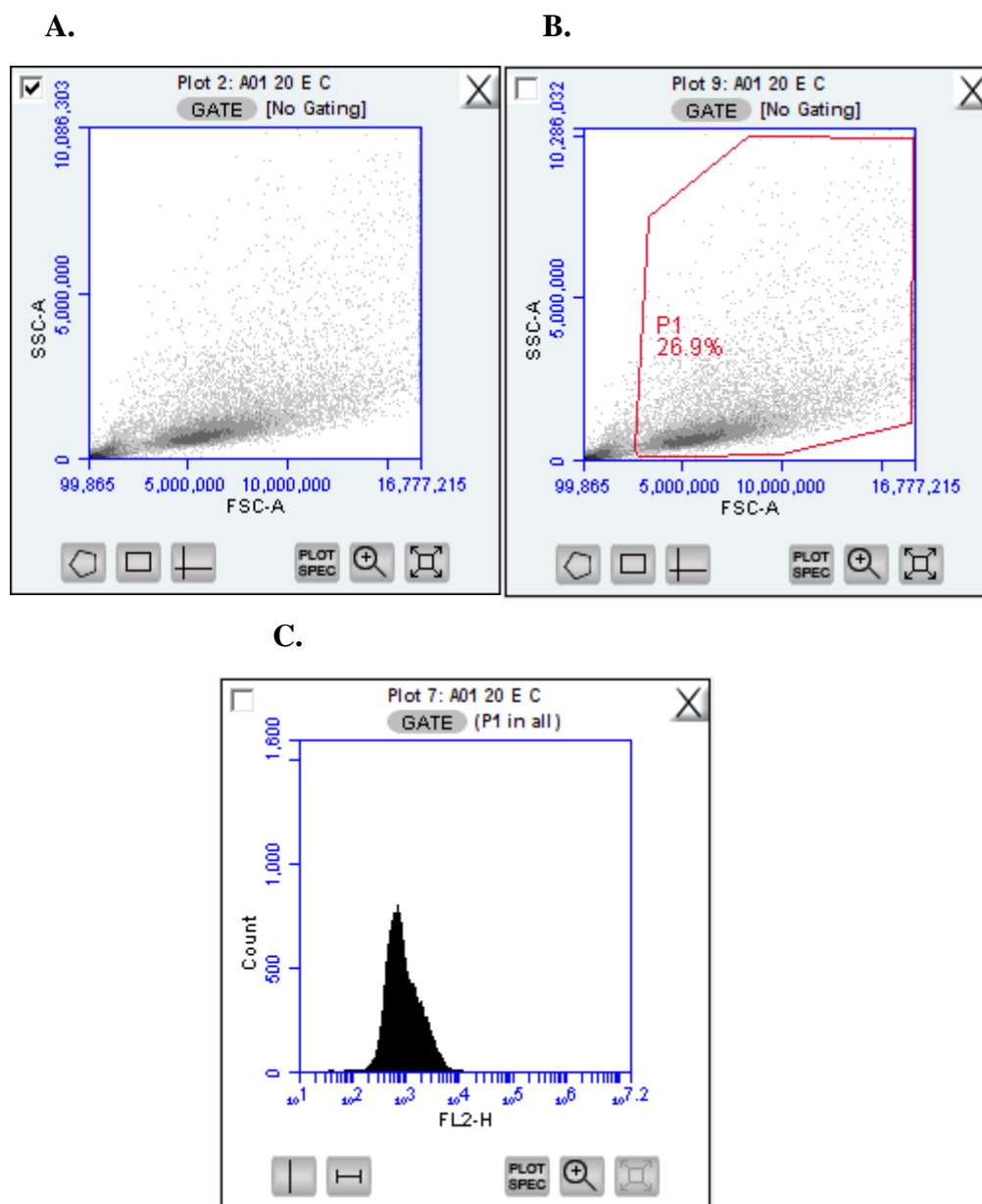
Figure A.3. Example views of BD CFlow software flow cytometry plots for controls.
BD CFlow software first displays frequency distribution plots with side scatter and forward scatter values of all 50,000 events recorded where each gray dot is considered an event or cell (A). Gating for live cells excludes events with low values for both forward and side scatter (B). These gated controls are then converted to a histogram of the number of times a fluorescent value is recorded (C) from which mean fluorescence is calculated.
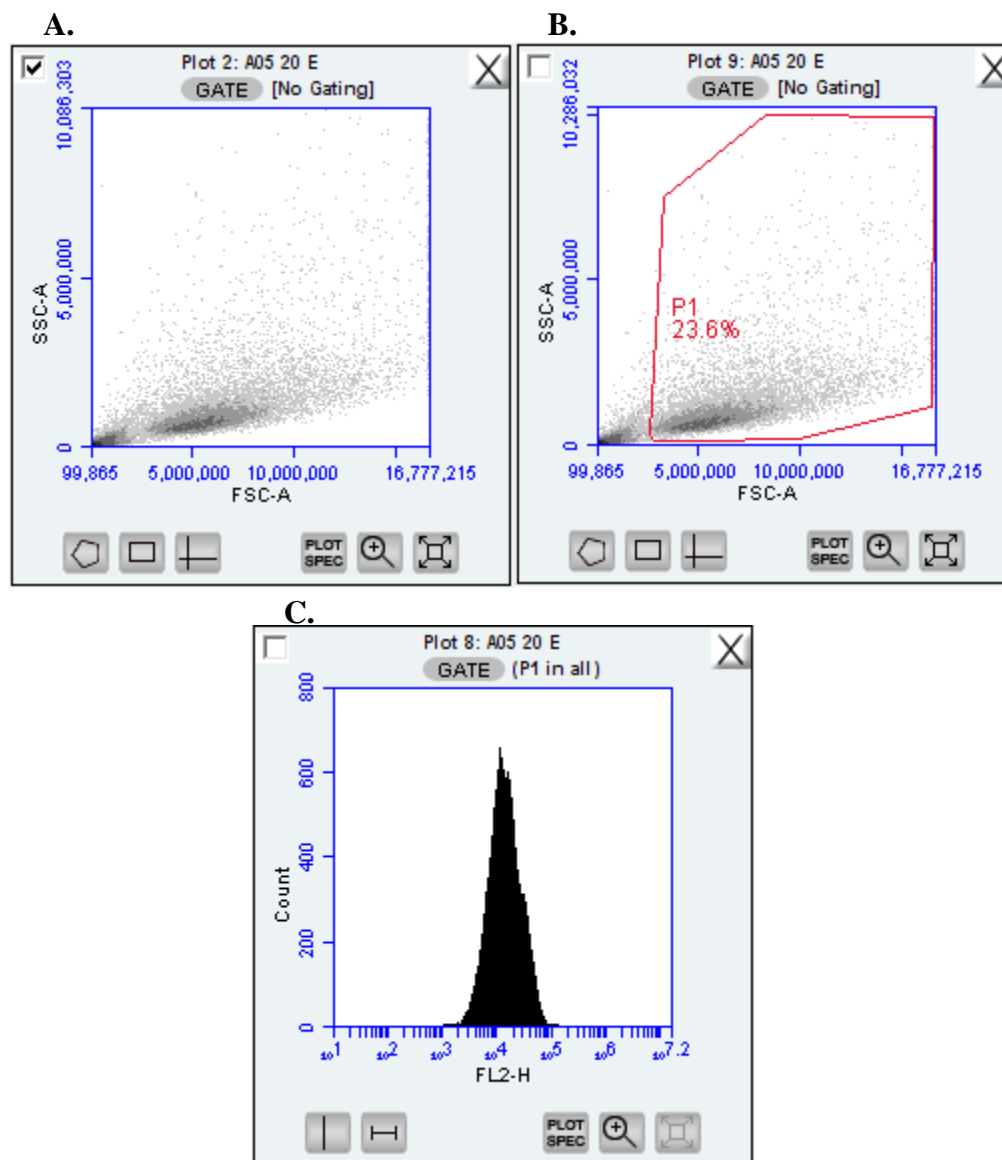
Figure A.4. Example views of BD CFlow software flow cytometry plots for samples treated with a fluorescent probe. BD CFlow software first displays frequency distribution plots with side scatter and forward scatter values of all 50,000 events recorded where each gray dot is considered an event or cell (A). Gating for live cells excludes events with low values for both forward and side scatter (B). This is the same gate that was applied to the control sample. These gated samples are then converted to a histogram of the number of times a fluorescent value is recorded (C) from which mean fluorescence is calculated.

Chapter 5: Reference List

Alberti K.G.M.M., Zimmet, P. and Shaw, J. (2004). The metabolic syndrome - a new worldwide definition. *Diabetes*, **366**: 1059-62.

Alvarez, S., Valdez, L.B., Zaobormyj, T. and Boveris, A. (2002). Oxygen dependence of mitochondrial nitric oxide synthase activity. *Biochem and Bioph Res Co,* **305**: 771-5.

Anderson, E.J. and Neufer, P.D. (2006). Type II skeletal myofibers possess unique properties that potentiate mitochondria H_2O_2 generation. *Am J Physiol Cell Physiol*, **290**: C844-51.

Ang, C.K., Tan, T.H., Walters, W.A.W. and Wood, C. (1969). Postural influence on maternal capillary oxygen and carbon dioxide tension. *Brit Med J*, **4**: 201-3.

Arbeille, P., Maulik, D., Fignon, A., Stale, H., Berson, M., Bodard, S. and Locatelli, A. Assessment of the fetal Po_2 changes by cerebral and umbilical doppler on lamb fetuses during acute hypoxia. *Ultrasound in Med and Biol*, **21**: 861-70.

Arthur, P.G., Giles, J.J. and Wakeford, C.M. (2000). Protein synthesis during oxygen conformance and severe hypoxia in the mouse cell line C2C12. *Biochem Medica*, **1475**: 83-9.

Barker, D.J.P. (2004). Developmental origins of adult health and disease. *J Epidemiol Community Health*, **58**: 114-5.

Barker, D.J.P., Martyn, C.N., Osmond, C., Hales, C.N. and Fall C.H.D. (1993). Growth *in utero* and serum cholesterol concentrations in adult life. *BMJ*: **307**: 1524-7.

Baschat, A.A. (2004). Fetal responses to placental insufficiency: an update. *BJOG-Int J Obstet Gy*, **111**: 1031-41.

Baschat, A.A., Galan, H.L., Bhide, A., Berg, C., Kush, M.L., Oepkes, D., Thilaganathan, B., Gembruch, U. and Harman, C.R. (2006). Doppler and biophysical assessment in growth restricted fetuses: distribution of test results. *Ultrasound Obstet Gynecol*, **27**: 41-7.

Baur, J.A. and Sinclair, D.A. (2006). Therapeutic potential of resveratrol: the *in vivo* evidence. *Nature Reviews*, **5**: 493-506.

Bazaes, R.A., Salazar, T.E., Pittaluga, E., Pena, V., Alegria, A., Iniguez, G., Ong, K.K., Dunger, D.B. and Mericq, M.V. (2003). Glucose and lipid metabolism in small for gestational age infants at 48 hours of age. *Pediatrics*, **111**: 804-9.

Bell, E.L., Klimova, T.A., Eisenbart, J., Moraes, C.T., Murphy, M.P., Budinger, G.R.S. and Chandel, N.S. (2007). The Qo site of the mitochondrial complex III is required for the transduction of hypoxic signaling via reactive oxygen species production. *J of Cell Biol*, **177**: 1029-1036.

Bergeron, R., Ren, J.M., Cadman, K.S., Moore, I.K., Perret, P., Pypaert, M., Young, L.H., Semenkovich, C.F. and Schulman, G.I. (2001). Chronic activation of AMP kinase results in NRF-1 activation and mitochondrial biogenesis. *Am J Physiol Endocrinol Metab*, **281**: E1340-6.

Biressi, S., Molinaro, M. and Cossu, G. (2007). Cellular heterogeneity during vertebrate skeletal muscle development. *Dev Bio*, **308**, 281-93.

Bristow, J., Rudolph, A.M., Itskovitz, J. and Barnes, R. (1983). Hepatic oxygen and glucose metabolism in the fetal lamb. *J Clin Invest*, **71**: 1047-61.

Brunelle, J.K., Bell, E.L., Queada, N.M., Vercauteren, K., Tiranti, V., Zeviani, M., Scarpulla, R.C. and Chandel, N.S. (2005). Oxygen sensing requires mitochondrial ROS but not oxidative phosphorylation. *Cell Metab*, **1**: 409-12.

Burattini, S., Ferri, P., Battistelli, M., Curci, R., Luchetti, F. and Falcieri, E. (2004). C2C12 murine myoblasts as a model of skeletal muscle development: morpho-functional characterization. *EJH*, **48**: 223-33.

Carroll, J., Fearnley, I.M., Shannon, R.J., Hirst, J. and Walker, J.E. (2003). Analysis of the subunit composition of complex I from bovine heart mitochondria. *Mol Cell Proteomics*, **2**: 117-26.

Cetin, I. and Alvino, G. (2009). Intrauterine growth restriction: Implications for placental metabolism and transport. A review. *Placenta*, **23**: S77-82.

Chan, S.Y., Zhang, Y., Hemann, C., Mahoney, C.E., Zweier, J.L. and Loscalzo, J. (2009). MicroRNA-210 control mitochondrial metabolism during hypoxia by repressing the iron-sulfur cluster assembly proteins ISCU1/2. *Cell Metab*, **10**, 273-84.

Chandel, N.S., Maltepe, E., Goldwasser, E., Mathieu, C.E., Simon, M.C. and Schumacker, P.T. (1998). Mitochondrial reactive oxygen species trigger hypoxia-induced transcription. *Proc Natl Acad Sci*, **95**: 11715-20.

Chandel, N.S., McClintock. D.S., Feliciano, C.E., Wood, T.M., Melendez. J.A., Rodriquez, A.M. and Schumacker, P.T. (2000). Reactive oxygen species generated at mitochondrial complex III stabilize hypoxia-inducible factor-1 during hypoxia. *J Biol Chem*, **275**: 25130-8.

Cooper, C.E. and Davies, N.A. (2000). Effects of nitric oxide and peroxynitrite on the cytochrome oxidase Km for oxygen: Implications for mitochondrial pathology. *Biochem Bioph*, **1459**: 390-6.

Cotney, J., Wang, Z. and Shadel, G.S. (2007). Relative abundance of the human mitochondrial transcription system and distinct roles for h-mtTFB1 and h-mtTFB2 in mitochondrial biogenesis and gene expression. *Nucleic Acids Research*, **35**: 4042-54.

Csiszar, A., Labinskyy, N., Pinto, J.T., Ballabh, P., Zhang, H., Losonczy, G., Pearson, K., de Cabo, R., Pacher, P., Zhang, C. and Ungvari, Z. (2009). Resveratrol induces mitochondrial biogenesis in endothelial cells. *Am J Physiol Heart Circ Physiol*, **297**: H13-20.

De Boo, H.A. and Harding J.E. (2006). The developmental origins of adult disease (Barker) hypothesis. *Aust NZ J Obstet Gynecol*, **46**: 4-14.

Duguez, S., Feasson, L., Denis, C. and Freyssenet, D. (2001). Mitochondrial biogenesis during skeletal muscle regeneration. *Am J Physiol Endocrinol Metab*, **282**: E802-9.

Finck, B.N. and Kelly, D.P. (2006). PGC-1 coactivators: inducible regulators of energy metabolism in health and disease. *J Clin Invest*, **116**: 615-22.

Ford, E.S., Giles, W.H. and Dietz, W.H. (2002). Prevalence of the metabolic syndrome among US adults: Findings from the third national health and nutrition exam survey. *Community Health*, **287**: 356-9.

Gillman, M.W. (2005). Developmental origins of health and disease. *New Engl J Med*, **353**: 1848-50.

Giussani, D.A., Salinas, C.E., Villena, M. and Blanco, C.E. (2007). The role of oxygen in prenatal growth: studies in the chick embryo. *J Physiol*, **585**: 911-17.

Gleyzer, N., Vercauteren, K. and Scarpulla, R.C. (2005). Control of mitochondrial transcription specificity factors (TFB1M and TFB2M) by nuclear respiratory factors (NRF-1 and NRF-2) and PGC-1 family coactivators. *Mol Cell Biol*, **25**: 1354-66.

Greijer, A.E. and van der Wall, E. (2004). The role of hypoxia inducible factor 1 (HIF-1) in hypoxia induced apoptosis. *J Clin Pathol*, **57**: 1009-14.

Guzy, R.D. and Schumacker, P.T. (2006). Oxygen sensing by mitochondria at complex III: the paradox of increased reactive oxygen species during hypoxia. *Exp Physiol*, **91**: 807-19.

Hales, C.N., Barker, D.J.P., Clark, P.M.S., Cox, L.J., Fall, C., Osmond, C. and Winter P.D. (1991). Fetal and infant growth and impaired glucose tolerance at age 64. *BMJ*, **303**: 1019-22.

Handschin, C. and Spiegelman, B.M. (2006). Peroxisome Proliferator-activated γ receptor coactivator 1 coactivators, energy homeostasis and metabolism. *Edocr Rev*, **27**: 728-35.

Heather, L.C., Cole, M.A., Tan, J., Ambrose. L.J.A., Pope, S., Abd-Jamil, A.H., Carter, E.E., Dodd, M.S., Yeoh, K.K., Schofield, C.J. and Clarke, K. (2012). Metabolic adaptation to chronic hypoxia in cardiac mitochondria. *Basic Res Cardiol*, **107**: 1-12.

Hendrix, N. and Berghella, V. (2008). Non-placental causes of intrauterine growth restriction. *Semin Perinatol*, **32**: 161-165.

Hoppeler, H., Vogt, M., Weibel, E.R. and Fluck, M. (2003). Response of skeletal muscle mitochondria to hypoxia. *Exp Physiol*, **88**: 109-19.

Ikizler, M., Ovali, C., Dernek, S., Erkasap, N., Sevin, B., Kaygisiz, Z. and Kural, T. (2006). Protective effects of resveratrol in ischemia-repurfusion injury of skeletal muscle: a clinically relevant animal model for lower extremity ischemia. *J Physiol*, **49**: 204-9.

Iossa, S., Mollica, M.P., Lionetti, L., Crescenzo, R., Botta, M. and Liverini, G. (2002). Skeletal muscle oxidative capacity in rats fed high-fat diet. *Obesity*, **26**: 65-72.

Jaquet, D., Gaboriau, A., Czernichow, P. and Levy-Marchal, C. Insulin resistance early in adulthood in subjects born with intrauterine growth retardation. *J Clin Endocr Metab*, **85**: 1401-06.

Joss-Moore, L.A., Metcalfe, D.B., Albertine, K.H., McKnight, R.A. and Lane R.H. (2010). Epigenetics and fetal adaptation to perinatal events: Diversity through fidelity. *J Anim Sci*, **88**: E216-22.

Kelley, D.E., He, J., Menshikova, E.V. and Ritov, V.B. (2002) Dysfunction of mitochondria in human skeletal muscle in Type 2 Diabetes. *Diabetes*, **51**: 2944-50.

Kelly, D.P. and Scarpulla, R.C. (2004). Transcriptional regulatory circuits controlling mitochondrial biogenesis and function. *Genes Dev*, **18**: 357-68.

Kim, K.W., Tchernyshyov, I., Semenza, G.L. and Dang, C.V. (2006). HIF-1-mediated expression of pyruvate dehydrogenase kinase: A metabolic switch required for cellular adaptation to hypoxia. *Cell Metab*, **3**: 177-85.

Koves, T.R., Usser, J.R. Noland, R.C., Slentz, D., Mosedale, M., Ilkayeva, O., Bain, J., Stevems, R., Dyck, J.R.B., Newgard, C.B., Lopaschuk, G.D. and Muoio, D.M. (2008). Mitochondria overload and incomplete fatty acid oxidation contribute to skeletal muscle insulin resistance. *Cell Metab*, **7**: 45-56.

Kulisz, A., Chen, N., Chandel, N.S., Shao, Z. and Schumacker, P.T. (2002). Mitochondrial ROS initiate phosphorylation of p38 MAP kinase during hypoxia in cardiomyocytes. *Am J Physiol Lung Cell Mol Physiol*, **282**: L1324-9.

Lackman, F., Capewell, V., Gagnon, R. and Richardson, B. (2001). Fetal umbilical cord oxygen values and birth to placental weight ratio in relation to size at birth. *Am J of Obstet Gynecol*, **185**: 674-82.

Lagouge, M., Argmann, C., Gerhart-Hines, Z., Meziane, H., Lerin, C., Daussin, F., Messadeq, N., Milne, J., Lambert, P., Elliot, P., Geny, B., Laakso, M., Puigserver, P. and Auwerx, J. (2006). Resveratrol improves mitochondrial function and protects against metabolic disease by activating SIRT1 and PGC-1α. *Cell*, **127**: 1109-22.

Lane, R.H., Chandorkar, A.K., Flozak, A.S. and Simmons, R.A. (1998). Intrauterine growth retardation alters mitochondrial gene expression and function in fetal and juvenile rat skeletal muscle. *Pediatric Research*, **43**: 563-70.

Lane, R.H., Maclennan, N.K., Daood, M.J., Hsu, J.L., Janke, S.M., Pham, T.D., Puri, A.R. and Watchko, J.F. (2003). IUGR alters postnatal rat skeletal muscle peroxisome proliferator-activated receptor- coactivator-1α gene expression in a fiber specific manner. *Pediatric Research*, **53**: 994-1000.

Lipsky, N.G. and Pedersen, P.L. (1981). Mitochondrial turnover in animal cells. *J Biol Chem*, **256**: 8652-7.

Livak, K.J. and Schmittgen, T. (2001). Analysis of relative gene expression data using real-time quantitative PCR and the $2^{-\Delta\Delta ct}$ Method. *Methods*, **25**: 402-8.

Liu, J., Chen, D., Yao, Y., Yu, B., Mao, X., He, J., Huang, Z. and Zheng, P. (2012). Intrauterine growth retardation increases the susceptibility of pigs to high-fat diet-induced mitochondrial dysfunction in skeletal muscle. *Plos One*, **7**: 1-13.

Mahal, H.S. and Mukherjee, T. (2006). Scavenging of reactive oxygen radicals by resveratrol: antioxidant effect. *Res Chem Intermed*, **32**: 59-71.

McLellan, K.C., Hooper, S.B., Bocking, A.D., Delhanty, P.J.D., Phillips, I.D., Hill, D.J. and Han, V.K.M. (1992). Prolonged hypoxia induced by the reduction of maternal uterine blood flow alters insulin-like growth factor-binding protein-1 (IGFBP-1) and IGFBP-2 gene expression in the ovine fetus. *Endocrinology*, **131**: 1619-28.

Menzies, R.A. and Gold, P.H. (1971). The turnover of mitochondria in a variety of tissues of young adult and aged rats. *J Biol Chem*, **246**: 2425-9.

Messina, G., Biressi, S., Monteverde, S., Magli, A., Cassano, M., Perani, L., Roncaglia, E., Tagliafico, E., Starnes, L., Campbell, C.E., Grossi, M., Goldhamer, D.J., Gronostajski, R.M. and Cossu, G. (2010). Nfix regulates fetal-specific transcription in developing skeletal muscle. *Cell*, **140**: 554-66.

Mootha, V.K., Handschin, C., Arlow, D., Xie, X., St. Pierre, J., Sihag, S., Yang, W., Altshuler, D., Puigserver, P., Patterson, N., Willy, P.J., Schulman, I.G., Heyman, R.A., Lander, E.S., Spiegelman, B.M. (2004). Err and Gabpa/b specify PGC-1α-dependent oxidative phosphorylation gene expression that is altered in diabetic muscle. *PNAS*, **101**: 6570-5.

Paddenberg, R., Ishaq, B., Goldenberd, A., Faulhammer, P., Rose, F., Weissman, N., Dullaeus-Braun, R.C. and Kummer, W. (2002). Essential role of complex II of the respiratory chain in hypoxia-induced ROS generation in the pulmonary vasculature. *Am J Physiol Lung Cell Mol Physiol*, **284**: L710-9.

Park, S.J., Ahmed, F., Philp, A., Baar, K., Williams, T., Luo, H., Ke, H., Rehmann, H., Taussig, R., Brown, A.L., Kim, M.K., Beaven, M.A., Burgin, A.B., Manganiello, V. and Chung, J.H. (2012). Resveratrol ameliorates aging-related metabolic phenotypes by inhibiting cAMP phosphodiesterases. *Cell*, **148**: 421-33.

Papandreou, I., Cairns, R.A., Fontana, L. Lim, A.L. and Denko, N.C. (2006). HIF-1 mediates adaptation to hypoxia by actively down-regulating mitochondrial oxygen consumption. *Cell Metab*, **3**: 187-97.

Pardi, G., Marconi, A.M. and Cetin I. (2002). Placental-fetal interrelationship in IUGR fetuses - A review. *Placenta*, **16**: S136-41.

Patti, M.E., Butte, A.J., Crunkhorn, S., Cusi, K., Berria, R., Kashyap, S., Miyazaki, Y., Kohane, I., Costello, M. Saccone, R., Landaker, E.J., Goldfine, A.B., Mun, E., DeFronzo, R., Finlayson, J., Kahn, R.C. and Mandaino, L.J. (2003). Coordinated reduction of genes of oxidative metabolism in humans with insulin resistance and diabetes: Potential role of PGC1 and NRF1. *PNAS*: **100**: 8466-71.

Petersen, K.F., Dufour, S., Befroy, D., Garcia, R. and Shulman, G.I. (2004). Impaired Mitochondrial activity in the insulin-resistant offspring of patients with Type 2 Diabetes. *N Engl J Med*, **350**: 664-71.

Peterside, I.E., Selak, M.A. and Simmons, R.A. Impaired oxidative phosphorylation in hepatic mitochondria in growth-retarded rats. *Am J Physiol Endocrinol Metab*, **285**: E1258-66.

Piruat, J.I. and Lopez-Barneo, J. (2005). Oxygen tension regulates mitochondrial DNA-encoded complex I gene expression. *J Biol Chem*, **280**: 42676-84.

Regnault, T.R.H., de Vrijer, B., Galan, H.L., Wilkening, R.B., Battaglia, F.C., Meschia, G. (2007). Development and mechanisms of fetal hypoxia in severe fetal growth restriction. *Placenta*, **28**: 714-23.

Regnault, T.R.H, Zhao, L., Chiu, J.S.S., Gottheil, S.K., Foran, A. and Yee, S.P. (2010). Peroxisome Proliferator-Activated Receptor -β/δ, -γ Agonists and Resveratrol Modulate Hypoxia Induced Changes in Nuclear Receptor Activators of Muscle Oxidative Metabolism. *PPAR research*, **2010**: 1-13.

Resnik, R. (2002). Intrauterine growth restriction. *Obstet Gynecol*, **99**: 490-6.

Sadiq, H.F., Das, U.G., Tracy, T.F. and Devaskar, S.U. (1999). Intra-uterine growth restriction differentially regulates perinatal brain and skeletal muscle glucose transporters. *Brain Research*, **823**: 96-103.

Scandurra, F.M. and Gnaiger, E. (2010). Cell respiration under hypoxia: Facts and artefacts in mitochondrial oxygen kinetics. *Advances in Exp Med and Bio*, **662**: 7-25.

Scarpulla, R.C. (2008). Transcriptional paradigms in mammalian mitochondrial biogenesis and function. *Physiol Rev*, **88**: 611-38.

Scarpulla, R.C. (2006). Nuclear control of respiratory gene expression in mammalian cells. *J of Cell Biochem*, **97**: 673-83.

Schreiber, S.N., Emter, R., Hock, M.B., Knutti, D., Cardenas, J., Podvinec, M., Oakeley, E.J. and Kralli, A. (2004). The estrogen-related receptor α (ERRα) functional in PPARgamma coactivator 1 (PGC-1)-induced mitochondria biogenesis. *Proc Natl Acad Sci*, **101**: 6472-7.

Schroedl, C., McClintock, D.S., Budinger, G.R.S. and Chandel, N.S. (2002). Hypoxic but not anoxic stabilization of HIF-1 requires mitochondrial reactive oxygen species. *Am J Physiol Lung Cell Mol Physiol*, **283**: L922-31.

Schuler, M., Ali, F., Chamon, C., Duteil, D., Bornert, J.M., Tardivel, A., Desvergne, B., Wahli, W., Chambon, P. and Metzger, D. (2006). PGC1α expression is controlled in skeletal muscles by PPARγ whose ablation results in fiber-type switching, obesity, and type 2 diabetes. *Cell Metab*, **4**: 407-14.

Seagroves, T.N., Ryan, H.E., Lu, H., Wouters, B.G., Knapp, M., Thibault, P., Laderoute, K. and Johnson, S. (2001). Transcription factor HIF-1 is a necessary mediator of the pasteur effect in mammalian cells. *Mol Cell Biol*, **21**: 3436-44.

Selak, M.A., Storey, B.T., Peterside, I., and Simmons R.A. (2003). Impaired oxidative phosphorylation in skeletal muscle of intrauterine growth-retarded rats. *Am J Physiol Endocrinol Metab*, **285**: 130-7.

Simmons, R.A., Templeton, L.J. and Gertz, S.J. (2001). Intrauterine growth retardation leads to the development of Type 2 Diabetes. *Diabetes*, **50**: 2279-86.

Simoneau, J. and Kelley D.E. (1997). Altered glycolytic and oxidative capacities of skeletal muscle contribute to insulin resistance in NIDDM. *J Appl Physiol*, **83**: 166-71.

Strauss, R.S. and Dietz, W.H. (1998). Growth and development of term children born with low birth weight: Effects of genetic and environmental factors. *J Pediatr*, **133**: 67-72.

Tello, D., Balsa, E., Acosta-Iborra, B., Fuertes-Yebra, E., Elorza, A., Ordonez, A., Corral-Escariz, M., Soro, I., Lopez-Bernardo, E., Perales-Clemente, E., Martinez-Ruiz, A., Enriquez, J.A., Aragones, J., Cadenas, S. and Landazuri, M.O. (2011). Induction of the mitochondrial NDUFA4L2 protein by HIF-1α decreases oxygen consumption by inhibiting complex I activity. *Cell Metab*, **14**, 768-79.

Terui, K., Haga, S., Enosawa, S., Onhuma, N. and Ozaki, M. (2004). Hypoxia/re-oxygenation-induced, redox-dependent activation of STAT1 (signal transducer and activator of transcription 1) confers resistance to apoptotic cell death via hsp70 induction. *Biochem J*, **380**: 203-9.

Timmers, S., Konings, E., Bilet, L., Houtkooper, R.H., van de Weijer, T., Goossens, G.H., Hoeks, J., van der Krieken, S., Ryu, D., Kersten, S., Moonen-Kornips, E., Hesselink, M.K.C., Kunz, I., Schrauwen-Hinderling, V.B., Blaak, E.E., Auwerx, J. and Schrauwen, P. (2011). Calorie restriction-like effects of 30 days of resveratrol supplementation on energy metabolism and metabolic profile in obese humans. *Cell Metab*, **14**: 612-22.

Turrens, J.F. (2003). Mitochondrial formation of reactive oxygen species. *J Physiol*, **552**: 335-44.

Vanden Hoek, T.L., Becker, L.B., Shao, Z., Li, C. and Schumacker, P.T. (1998). Reactive oxygen species released from the mitochondria during brief hypoxia induce preconditioning in cardiomyocytes. *J Biol Chem*, **273**: 18092-18098.

World Health Organization (2004). Low birthweight: Country, regional and global estimates. *WHO*, 1-27.

Yun, Z., Lin Q. and Giaccia, A.J. (2005). Adaptive myogenesis under hypoxia. *Mol Cell Biol*, **25**: 3040-55.

Zhu M.J., Ford, S.P., Means, W.J., Hess, B.W., Nathanielsz, P.W. and Du, M. (2006). Maternal nutrient restriction affects properties of skeletal muscle in offspring. *J Physiol*, **575**: 241-50.

Zong, H., Ren, J.M., Young, L.H., Pypaert, M., Mu, J., Birnbaum, M.J. and Shulman, G.I. (2002). AMP kinase is required for mitochondrial biogenesis in skeletal muscle in response to chronic energy deprivation. *PNAS*, **99**: 15983-7.

Zuo, L. and Clanton, L. (2005). Reactive oxygen species formation in the transition to hypoxia in skeletal muscle. *Am J Physiol Cell Physiol*, **289**: C207-16.

KATHLEEN BELGRAVE

EDUCATION

University of Western Ontario, London, ON
September 2010 - Current
• M.Sc. with focus in Biology (Completion date: July 2012)
• Current research: Hypoxia-induced alterations in skeletal muscle cell respiration

University of Western Ontario, London, ON
September 2006 - April 2010
• Graduated with an Honours Bachelor of Science in Biology and Physiology
• Dean's Honour List for 3 years of Undergraduate Degree

AWARDS AND ACADEMIC ACHIEVEMENTS

Scholarships
Western Graduate Research Scholarship, September 2010 - April 2012
Western Scholarship of Excellence, September 2006 - April 2007

Published Manuscript
• Brown, J.C.L., Chung, D.J., **Belgrave, K.R.** and Staples, J.F. (2011). Mitochondrial metabolic suppression and reactive oxygen species production in liver and skeletal muscle of hibernating thirteen-lined ground squirrels. *Am J Physiol,* **1**: R15-R28

Conference Presentations
• Poster Presentation of current research:
    - Lawson Research Day, London, ON (local)
    - Developmental Origins of Health and Disease, Portland, OR (international)
    - Perinatal Investigator Meeting, Kingston, ON (national)
• PowerPoint presentation of current research:
    - Obstetrics and gynaecology research day, London, ON (local)

VOLUNTEER WORK

Mentor for 4th year thesis student including instruction in laboratory techniques
September 2011 - April 2012